Staphylococcal Nuclease: Sequential Assignments and Solution Structure†

Dennis A. Torchia,*,‡ Steven W. Sparks,‡ and Ad Bax§

Bone Research Branch, National Institute of Dental Research, and Laboratory of Chemical Physics, National Institute of Diabetes and Digestive and Kidney Diseases, National Institutes of Health, Bethesda, Maryland 20892

Received December 12, 1988; Revised Manuscript Received March 8, 1989

ABSTRACT: Sequential assignments are reported for backbone ^{15}N and ^{1}H of nearly all residues of staphylococcal nuclease (Nase) complexed with thymidine 3′,5′-diphosphate and Ca^{2+}. Because of the relatively large size of the Nase ternary complex, M_r 18K, the crucial element of our assignment strategy was the use of isotope-edited two-dimensional NMR spectra, particularly ^{15}N-edited nuclear Overhauser enhancement spectroscopy (NOESY), ^{15}N-edited *J*-correlated spectroscopy (COSY), and $^{1}H/^{15}N$ or $^{1}H/^{13}C$ heteronuclear multiple quantum shift correlation spectroscopy (HMQC). These experiments, together with the more conventional NOESY, COSY, and homonuclear Hartmann–Hahn spectra of natural abundance or deuteriated samples, yielded backbone assignments of 127 of the 136 residues in the structured part of the protein. Using the NOESY data, we identified three helical domains and several β-sheets which were in close correspondence with secondary structure identified in the crystal structure. Moreover, many long-range NOESY connectivities were identified that were in agreement with distances derived from the crystal structure. The region of the sequence in the neighborhood of residue 50 appears to be more flexible and disordered in solution than in the crystal. Very slowly exchanging amide protons are those found to be hydrogen bonded in the crystal structure; however, even hydrogen-bonded amides located within similar types of regular secondary structures, e.g., α-helices, exchange with greatly different rates.

Staphylococcal nuclease, Nase,[1] is an enzyme that is well suited for structure–function studies (Tucker et al., 1978, 1979a–c). As a result of the successful expression of the Nase gene in *Escherichia coli* (Shortle, 1983; Calderon et al., 1985; Evans et al., 1987), there is great current interest in studying the biochemical and physical properties of the wild-type and mutant enzymes in solution and in the crystalline state (Calderon et al., 1985; Shortle & Lin, 1985; Fox et al., 1986; Evans et al., 1987; Hibler et al., 1987; Serpersu et al., 1987). High-resolution nuclear magnetic resonance spectroscopy can provide detailed information about protein structure and dynamics (Wuethrich, 1986; Ernst et al., 1987), once NMR signals have been assigned. Although backbone amide nitrogen and proton signals of residues in Nase α-helices (Torchia et al., 1988a,b) and histidine side chain signals (Alexandrescu et al., 1988) have been assigned, the bulk of the Nase proton and heteroatom signals are not yet assigned, greatly limiting the information that one can obtain from NMR experiments.

Herein we report assignments of backbone nitrogens and protons in the structured domains of the protein, consisting of the nonterminal residues 6–141. Assignments of about one-third of the side-chain protons are also reported. We chose to study the protein complexed with Ca^{2+} and pdTp because, when we began this work, crystal coordinates were available only for this form of the enzyme, and one objective of our work is to compare solution and crystal structures of Nase. Although Redfield and Dobson (1988) have assigned hen lysozyme without recourse to isotopic labeling, it is widely recognized that sequential assignments of proteins are greatly facilitated by incorporation of isotopically enriched amino acids into proteins (Kainosho & Tsuji, 1982; Cross & Opella, 1985; Griffey et al., 1985, 1986, 1987; McIntosh et al., 1987, 1988; Leighton & Lu, 1987; Senn et al., 1987; LeMaster & Richards, 1988; Torchia et al., 1988a,b; Oh et al., 1988; Westler et al., 1988). We have prepared a large number of Nase samples containing amino acids enriched with ^{2}H, ^{13}C, or ^{15}N. Heteronuclear multiple quantum shift correlation, HMQC, spectroscopy (Mueller, 1979; Bax et al., 1983; Bendall et al., 1983; Griffey & Redfield, 1987) and isotope-edited NOESY spectroscopy (McIntosh et al., 1987; Senn et al., 1987; Fesik et al., 1988) of ^{13}C-, ^{15}N-, and 1-$^{13}C/^{15}N$-labeled samples were used to obtain backbone-type assignments and sequential assignments. These spectra together with NOESY, COSY, and HOHAHA spectra (Wuethrich, 1986; Bax & Lerner, 1986; Ernst et al., 1987) of natural abundance and partially deuteriated samples provided sequential assignments of backbone protons and nitrogen nuclei in 127 out of the 136 residues in the structured part of Nase.

Using these assignments, we have identified a large number of sequential and long-range NOESY connectivities that allow us to compare many aspects of the protein structure in solution with the crystal structure. In addition we have identified the most stable parts of the protein structure on the basis of the criterion of very slow hydrogen exchange. Beyond these two examples, the assignments should enable other investigators to carry out detailed NMR studies of the structure and dynamics of wild-type and mutant Nase samples.

† This work was supported by the AIDS Targeted Antiviral Program of the Office of the Director of the National Institutes of Health.

‡ Bone Research Branch.

§ Laboratory of Chemical Physics.

[1] Abbreviations: Nase, staphylococcal nuclease; pdTp, thymidine 3′,5′-diphosphate; NMR, nuclear magnetic resonance; NOE, nuclear Overhauser effect; COSY, two-dimensional correlation spectroscopy; HOHAHA, two-dimensional homonuclear Hartmann–Hahn spectroscopy; NOESY, two-dimensional NOE spectroscopy; HMQC, two-dimensional heteronuclear multiple quantum shift correlation spectroscopy; HMBC, two-dimensional heteronuclear multiple bond correlation spectroscopy; PS COSY, pseudo-single-quantum COSY spectroscopy; Z, either Glu or Gln; B, either Asp or Asn; [^{2}H]TSP, sodium [2,2,3,3-$^{2}H_4$]-3-(trimethylsilyl)propionate.

This article not subject to U.S. Copyright. Published 1989 by the American Chemical Society

Table I: Listing of Residues Labeled at the Peptide Nitrogen and the Peptide Carbonyl Carbon in the Different Labeled Nase Samples

^{15}N	1-^{13}C	mg of L-amino acid/L of M9
Ala	Lys	A, 250; K, 100
Glu	Pro	E, 85; P, 90
Glu	Val	E, 85; V, 160
Met	Lys	M, 70; K, 80
Met	Leu	M, 90; L, 70
Leu		L, 70
Phe	Ala	F, 100; A, 225
Ser	Trp	S, 80; W, 20
Tyr	Ile	Y, 60; I, 50
Val	Leu	V, 60; L, 50
His, Phe	Thr	H, 20; F, 60; T, 30
Leu, Ser	Lys	L, 80; S, 125; K, 80
Lys, Tyr	Ala	K, 100; Y, 60; A, 250
Thr, Tyr	Met	T, 30; Y, 60; M, 60
His, Ile, Leu	Leu	H, 10; I, 50; L, 25
Gly, Ile, Ser, Tyr	Lys	G, 200; I, 50; Y, 60; K, 100
all residues		

Table II: Listing of Residues Labeled at Aliphatic Carbon Sites in the Different Enriched Nase Samples

residue	label	residue	label
Ala	3-^{13}C	Ser	2-^{13}C
Gly	2-^{13}C	Thr	3,4-$^{13}C_2$
Phe	2-^{13}C	Tyr	3-^{13}C
Pro	2-^{13}C		

Materials and Methods

Nase samples were obtained from transformed *Escherichia coli* (strain N4830) provided by Professor John Gerlt, University of Maryland, containing the expression plasmid pNJS (Hibler et al., 1987). The labeled enzyme was prepared according to procedures described by Hibler et al. (1987), except that the amounts of the individually labeled amino acids added to the M9 medium just prior to thermal induction are those listed in Table I. In the cases of Val, Ile, and His, which are growth requirements, about 40% of the indicated amounts were added at induction and the rest to the growth medium.

A listing of the ^{15}N- and ^{13}C-labeled Nase samples is given in Tables I and II. All labeled amino acids were obtained from commercial sources except for D,L-[3,4-^{13}C]threonine and D,L-[^{15}N,1-^{13}C]leucine, which were synthesized by Professor Paul Young, CUNY. Carbon-13 spectra of acid-hydrolyzed ^{13}C-labeled Nase samples showed no evidence of cross-labeling except from Gly into Ser. One unexpected observation occurred when a medium containing [2-^{13}C]Gly and no Ser yielded a protein not only labeled with [2-^{13}C]Gly and [2-^{13}C]Ser but labeled with [3-^{13}C]Ser as well, Figure 2Sa (see paragraph at end of paper regarding supplementary material).

Although scrambling of ^{15}N by transamination is not uncommon when *E. coli* proteins are being labeled (Muchmore et al., 1989), we observed strong cross-labeling only from Ser to Gly and from Glu to Gln in our initial set of HMQC spectra (Torchia et al., 1988b). As we built up our library of HMQC spectra, it became clear that weak signals observed in many HMQC spectra, Figures 2 and 1S, resulted from cross-labeling; e.g., the weak Val signals identified in Figure 2b result from cross-labeling. Fortunately, because the cross-labeling levels were low and involved relatively few amino acids, we could identify the cross-labeled peaks by comparing the HMQC spectra of the various ^{15}N-labeled Nase samples. Occasionally cross-labeling proves to be a benefit when sequential assignments are being made. For instance, after Figure 2a was used to identify the weak Ala signals in the HMQC spectrum of Nase labeled with [^{15}N]Glx, it became clear early in the assignment process that the cross-peaks having intensities of ca. 40% that of the Glx signals were due to cross-labeled Asx residues. In this way we obtained nearly all the Asx-type assignments without having to prepare a separate Asx-labeled sample.

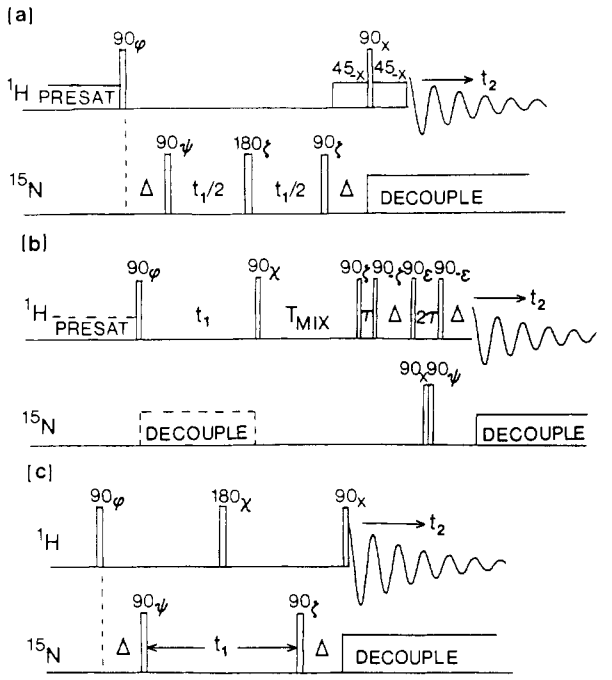

FIGURE 1: Pulse sequences of (a) the PS COSY experiment, (b) the edited NOESY experiment, and (c) the HMQC–COSY experiment (Clore et al., 1988). In all three pulse schemes the delay Δ is 4 ms, slightly shorter than $1/(2J_{NH})$. (a) When conducted in H_2O solution, water presaturation is necessary. Phase cycling is as follows: ϕ = $x, -x$; ψ = $2(x), 2(-x)$; ζ = $4(x), 4(-x)$; Acq = $x, -x, -x, x, -x, x, x, -x$. The phase ϕ is incremented 90° in successive t_1 increments, TPPI (Marion & Wuethrich, 1983). (b) Implementation depended upon the spectrometer used. On the AM-600 presaturation was not used, and the carrier was positioned exactly on the water resonance with χ fixed at 45°. The 45° phase shift prevents complete inversion of the water resonance during each individual scan. Radiation damping, due to the strong tranverse component of the water magnetization, rapidly drives the water magnetization to the z axis during the NOE mixing time, T_{MIX}. On the AM-600 phase cycling was as follows: ϕ = $8(x), 8(-x)$; ζ = $4(x), 4(y), 4(-x), 4(-y)$; ϵ = $x, y, -x, -y, y, -x, -y, x, -x, -y, x, y, -y, x, y, -x$; ψ = $16(x), 16(-x)$; Acq = $2(x,-x), 2(y,-y), 2(x,-x), 2(y,-y), 2(-x,x), 2(-y,y), 2(-x,x), 2(-y,y)$. The phase ϕ is incremented 90° in successive t_1 increments, TPPI. On the NT-500, a weak (γB_2 ca. 10 Hz) presaturating field was required in addition to the 1–1 echo read sequence (Roy & Redfield, 1984; Sklenar & Bax, 1987), and the phase cycling was as follows: ϕ = $x, y, -x, -y$; ζ = x; ϵ = $4(x), 4(y), 4(-x), 4(-y)$; ψ = $16(x), 16(-x)$; Acq = $2(x), 4(-x), 4(x), (4-x), 2(x), 2(-x), 4(x), 4(-x), 4(x), 2(-x)$. Data for odd- and even-numbered scans were stored in separate memory locations, and data were processed following the protocol of States et al. (1982). ^{15}N decoupling during t_1 was used in some of the edited NOESY experiments. (c) Phase cycling was as follows: ϕ = x; ψ = $x, y, -x, -y$; χ = $4(x), 4(y), 4(-x), 4(-y)$; ζ = $16(x), 16(-x)$; Acq = $2(x), 4(-x), 4(x), 4(-x), 2(x), 2(-x), 4(x), 4(-x), 4(x), 2(-x)$. Data for odd- and even-numbered scans were stored in separate memory locations.

Samples of fully ^{15}N-labeled Nase were prepared by growing the N4830 *E. coli* in supplemented M9 media (Hibler et al., 1987) containing [^{15}N]ammonium chloride, Merck Inc., and withholding all amino acids except D,L-[^{15}N]His (30 mg/L), L-[^{15}N]Ile/allo-L-[^{15}N]Ile (60 mg/L), and [^{15}N]Val (60 mg/L). The N4830 strain is an Ile/Val auxotroph, and grows very slowly without His.

Two types of deuteriated Nase samples were prepared. The first sample was obtained from *E. coli* grown on supplemented M9 medium (Hibler et al., 1987) containing 100% H_2O and 0.6 g/L perdeuteriated amino acids (except for Trp which was

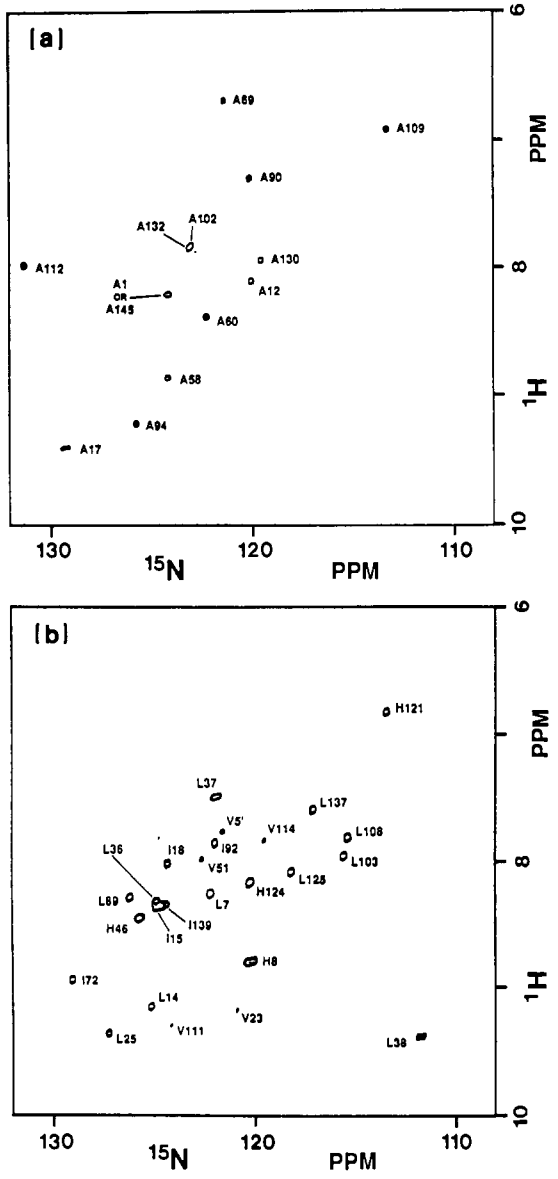

FIGURE 2: 500-MHz ^1H–^{15}N HMQC spectra of Nase labeled with (a) [1-^{13}C]K/[^{15}N]A, pH 7.0, and (b) [1-^{13}C,^{15}N]L/[^{15}N]H/[^{15}N]I, pH 7.0. The signal assignments given in these and subsequent spectra are discussed in the text. Note the low-level cross-labeling into Val in (b).

protiated at the α- and β-carbons), Merck Inc. A variety of one- and two-dimensional NMR spectra showed that the average level of deuteriation was 60–70% at backbone carbons and 85–95% on side-chain carbons. Asx, Ala, Gly, Glx, and Ser residues showed higher than average levels of protiation at α-carbons and particularly at β-carbons than other residues. A second sample of deuteriated Nase was prepared in the same manner as described above except that [^{15}N,^1H]Val and [^{15}N,^1H]Met were added to the M9 media just before induction of Nase synthesis. This permitted straightforward identification of many Val and Met protons in HOHAHA and NOESY spectra.

As a consequence of the plasmid construction (Fox et al., 1986; Hibler et al., 1987) of the Nase plasmid, the Nase produced by the *E. coli* has a heptapeptide appended to the N-terminus. The seven residues in this sequence are numbered 1′–7′. These residues as well as the first five residues and the last eight residues in the wild-type sequence are disordered and highly flexible and have no known role in the structure or function of the protein. For these reasons we did not make a strong effort to assign these terminal residues; rather, they were assigned as a byproduct of the sequential assignments of residues in the structured domain of Nase. The terminal residue assignments are summarized in Tables IS and IIS.

NMR spectra were recorded on Nase solutions having the following composition: NaCl, 100 mM; Nase, 1.5–2.0 mM; pdTp, 5 mM; $CaCl_2$, 10 mM; borate buffer, 50 mM. The pH meter readings of the Nase solutions were in the range 6.5–7.5, and the sample temperatures were in the range 36–38 °C.

Spectra were recorded on a modified NT 500 spectrometer and on a Bruker AM600 spectrometer. The typical spectrometer settings used to record HMQC and NOESY spectra at 500 MHz are given by Torchia et al. (1988a,b). The pulse schemes used to record PS COSY, edited NOESY, and HMQC-COSY experiments are shown in Figure 1. Proton chemical shifts are relative to the water signal (4.67 ppm relative to TSP in H_2O at 36.5 °C). ^{15}N and ^{13}C chemical shifts are relative to external ammonia and TSP, respectively. Uncertainties in chemical shifts are 0.02 and 0.1 ppm for protons and heteronuclei, respectively. All chemical shifts listed in Table III were derived from spectra recorded at pH 7.4.

Results

Assignments of NH Protons and α-Protons to Amino Acid Residue Types. In the standard method of protein sequential assignments (Wuethrich, 1986) one first assigns signals to amino acid residue types by means of *J*-connectivity patterns observed in COSY, RELAY COSY, and/or HOHAHA spectra. Unfortunately, because Nase tumbles slowly, $1/T_2$ is considerably larger than many proton three-bond *J*-couplings, resulting in a substantial loss in sensitivity in these *J*-correlated experiments. In addition, because of the large number of protons in Nase, many connectivities are not clearly resolved in natural abundance spectra.

Because of the sensitivity and resolution problems encountered in natural abundance spectra, we use isotopically enriched samples to obtain many of the backbone-type assignments. Amide nitrogen and amide proton type assignments are obtained for all residues except Arg and Trp from $^1H/^{15}N$ HMQC spectra of Nase samples, Table I, containing ^{15}N-labeled amino acids, Figures 2 and 1S. The $^1H/^{15}N$ correlations of the Asx residues occur as low-intensity signals in the HMQC spectrum of [^{15}N]Glx-labeled Nase, Figure 1Sa, as a consequence of cross-labeling. The amide proton of W140 is assigned as part of the Trp spin system identification presented below.

The aliphatic protons of a number of types of amino acids are identified in HMQC spectra, Figures 3 and 2S, of Nase samples, Table II, containing amino acids enriched in ^{13}C. In a few cases HMQC–HOHAHA relay spectra (Lerner & Bax, 1986) are used to obtain α–β proton correlations.

Identification of Ala, Gly, and Ser Spin Systems. The HOHAHA spectrum, Figure 4, confirms the previous identification (Torchia et al., 1988b) of the intraresidue Ala α–β connectivities. In addition to the seven intraresidue Ala N–β connectivities previously assigned (Torchia et al., 1988b), five N–β connectivities are identified in the NOESY spectrum of deuteriated Nase, Figure 5, by use of the information available from the HMQC spectra of Nase labeled with [3-^{13}C]Ala (Torchia et al., 1988b) or with [^{15}N]Ala, Figure 2a. As noted previously (Torchia et al., 1988b), methyl groups of Ala residues are the only methyl groups that are significantly protiated in the deuteriated Nase sample. The NH–α connectivities of the 12 identified Ala spin systems are observed in the PS COSY spectrum, Figure 6. NH–α connectivities have not been observed for two Ala spin systems; however, their

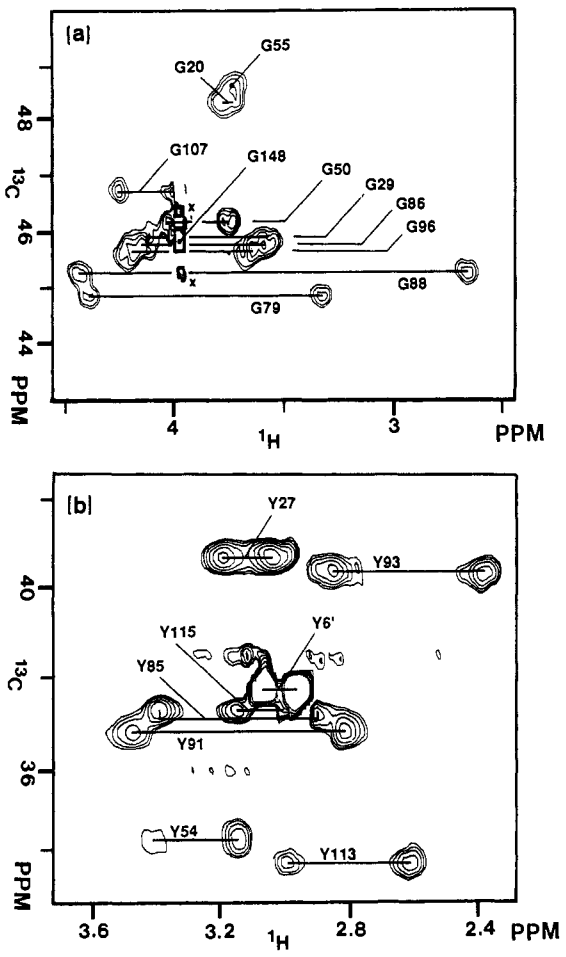

FIGURE 3: 500-MHz ^{1}H–^{13}C HMQC spectra of Nase labeled with (a) [2-^{13}C]G, pH 6.5, and (b) [3-^{13}C]Y, pH 7.0.

N–β connectivities have been identified in a ^{1}H–^{15}N HMBC spectrum (Bax et al., 1988). These spin systems are assigned to A1 and A145, which reside in the disordered terminal domains of Nase, because their aliphatic protons have large T_2 values and random coil shifts (Wuethrich, 1986; Howarth & Lilley, 1978).

The NH protons and α-protons of the 10 Gly residues are observed in HMQC spectra of Nase labeled with [^{15}N]Gly, Figure 1Sb, and [2-^{13}C]Gly, Figure 3a. The off-diagonal Gly α–α cross-peaks are observed in HOHAHA, Figure 4, and COSY and NOESY spectra (not shown). The Gly NH–α spin system identifications are made by combining the information obtained from the HMQC spectra with connectivities observed in PS COSY spectra (Bax et al., 1988a), ^{15}N-edited NOESY spectra, and NOESY spectra, Figures 5, 6, 7a, and 8. The NH protons and α-protons of one Gly residue (a) lack NOESY connectivities, (b) have large T_2 values, and (c) have random coil chemical shifts and are therefore assigned to G148, the only Gly residue located in the disordered C-terminus of Nase.

Three of the six Ser α-proton signals observed in the HMQC spectrum of Nase labeled with [2-^{13}C]Ser, Figure 2Sa, have large T_2 values and random coil shifts and are assigned to the three Ser residues in the terminal domains of Nase. The remaining three Ser α-signals are correlated to the three Ser NH signals, observed in the HMQC spectrum, Figure 1Sb, of Nase labeled with [^{15}N]Ser, by connectivities observed in the edited NOESY spectrum, Figure 7a, of Nase labeled with [^{15}N]Ser. These assigned correlations are reinforced by the identification of the three Ser NH–α connectivities in the PS COSY spectrum, Figure 6.

Identification of Thr and Val Spin Systems. Having identified the 14 Ala α–β connectivities in the Nase HOHAHA spectrum, Figure 4, we identify the aliphatic protons of the 11 Thr spin systems on the basis of their unique α–β–γ HOHAHA connectivity patterns and the Thr β- and γ-shifts observed in the HMQC spectrum of Nase containing [3,4-^{13}C]Thr, Figure 2Sb,c. Only the α-proton of T41 was not identified by this means, and it was found at 5.20 ppm in the HMBC spectrum of Nase labeled with [1-^{13}C]Thr (Bax et al., 1988). The three sets of Thr aliphatic spin systems having large T_2 values and random coil chemical shifts are assigned to the T2′, T2, and T4 residues in the terminal regions of Nase. The NH–α connectivities of these residues have not been identified. The NH–α connectivities of seven of the remaining eight Thr residues are identified by combining aliphatic proton shift information with the Thr NH shifts obtained from the

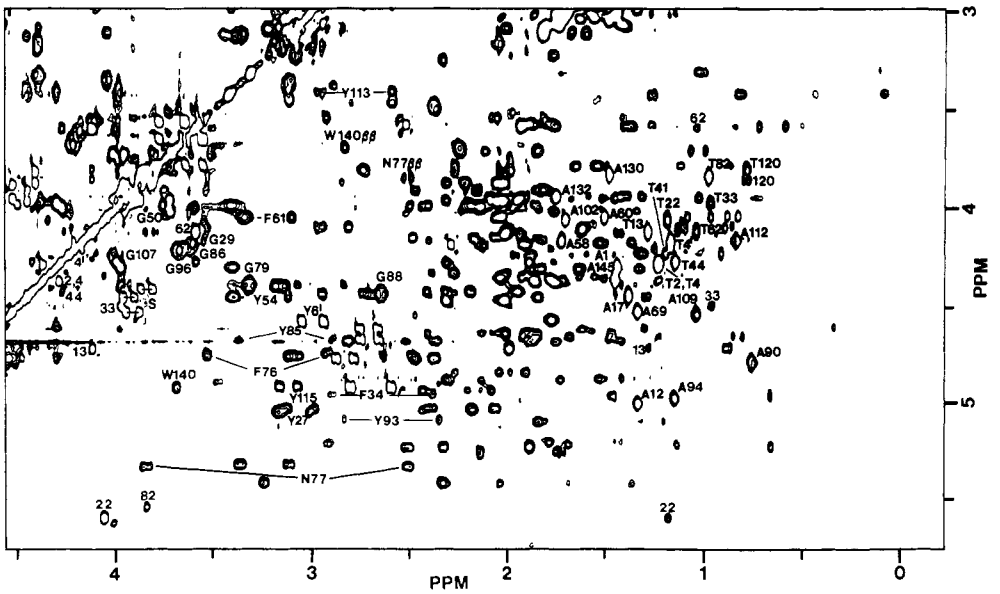

FIGURE 4: Portion of the 600-MHz aliphatic HOHAHA spectrum of Nase in ^2H_2O solution. Mixing time, 35 ms; pH 7.4. The Gly α–α, Ala α–β, aromatic α–β, and Thr β–γ connectivities are identified by the one-letter amino acid code followed by the residue number. The Thr α–β and β–γ connectivities are identified by residue number only, and the three α–β connectivities of the three Ser residues in the unstructured terminal domains are labeled with the single letter S.

Table III: Assignments of Staphyloccal Nuclease[a]

residue	^{15}NH	NH	αH	βH	γH and other H	residue	^{15}NH	NH	αH	βH	γH and other H
K6			4.39			F76	126.6	8.83	4.75	2.93, 3.53	δH 7.70; εH 7.27; ζH 6.79
L7	122.2	8.24	4.56								
H8	119.6	8.76	4.92			N77	123.2	9.23	5.33		
K9	123.9	8.30	4.87			K78	119.1	10.22	4.23		
E10	123.2	9.38	5.04			G79	110.8	8.67	3.32, 4.37		
P11			4.93			Q80	124.8	8.74	4.17		
A12	120.0	8.11	4.99	1.33		R81	120.2	8.59			
T13	108.8	8.11	4.72	4.12	γH 1.28	T82	107.8	7.34	5.53	3.84	γH 0.97
L14	125.1	9.14	4.14			D83	121.6	8.82			
I15	124.6	8.34	4.23			K84	125.3	8.72	4.06		
K16	114.4	8.06	4.44			Y85	120.6	8.23	4.68	2.88, 3.37	δH 7.02; εH 6.95
A17	129.4	9.42	4.44	1.41		G86	109.3	8.25	3.61, 4.18		
I18	124.3	8.02	4.10			R87	121.6	8.73	4.40		
D19	119.0	8.59	4.77			G88	108.3	8.82	2.64, 4.43		
G20	103.8	8.91	3.71, 3.75			L89	126.1	8.27	5.22		
D21	111.8	7.54	4.89			A90	120.1	7.32	4.81	0.77	
T22	117.6	7.70	4.89	4.06	γH 1.18	Y91	122.7	9.07	4.62	2.78, 3.46	δH 7.15,[c] 7.46; εH 6.57; ζH 9.67
V23	120.7	9.17	4.65	1.92	γH 0.79, 0.84						
K24	127.3	9.43	5.43			I92	122.0	7.84	4.97		
L25	127.3	9.37	5.20			Y93	126.3	9.54	5.10	2.35, 2.82	δH 6.64; εH 6.74
M26	122.1	9.56	4.88			A94	125.8	9.22	4.98	1.16	
Y27	129.6	9.05	5.04	3.01, 3.18	δH 7.34; εH 6.91	D95	127.5	9.71	4.43		
K28	127.5	9.29	3.59			G96	103.1	9.38	3.67, 4.22		
G29	102.4	8.42	3.56, 4.09			K97	121.3	7.87	5.07		
Q30	119.3	7.83	5.03			M98	126.6	9.23	3.80		
P31			4.84			V99	136.2	10.20	3.71	1.84	γH 0.98, 1.06
M32	125.7	9.57	4.65			N100	108.2	9.65	4.09		
T33	124.2	8.90	4.50	3.97	γH 0.95	E101	112.6	6.19	3.68		
F34	125.8	9.73	4.94	2.38, 2.91	δH 6.93; εH 6.91; ζH 6.64	A102	123.1	7.83	4.06	1.73	
R35	124.7	9.84	4.98			L103	115.5	7.95	3.34		
L36	124.8	8.31	4.36			V104	117.0	6.88	3.94	2.08	γH 1.01, 1.02
L37	121.9	7.47	3.95			R105	122.5	9.12	4.12		
L38	111.6	9.37	4.34			Q106	112.1	7.09	4.33		
V39	103.8	6.98	5.75	1.87	γH 0.73, 1.01	G107	106.8	8.02	3.98, 4.24		
D40	119.2	8.89	5.21			L108	115.3	7.79	4.29		
T41	119.6	9.50	5.20	4.23	γH 1.18	A109	113.1	6.92	4.55	1.05	
P42						K110	117.3	7.54	5.10		
E43						V111	124.1	9.28	4.72	1.99	γH 0.87, 0.89
T44			4.43	4.27	γH 1.14	A112	131.3	7.98	4.17	0.83	
K45			4.31			Y113	110.3	7.82	3.42	2.59, 2.97	δH 6.98; εH 6.74
H46	125.5	8.44	4.76			V114	119.4	7.82	3.58	1.93	γH 0.57, 0.71
P47						Y115	130.5	9.04	5.03	2.99, 3.13	δH 7.17; εH 6.61
K48						K116	116.0	7.82			
K49						P117					
G50	109.1	8.17	3.74, 3.97			N118	128.6	8.68	5.32		
V51	122.3	7.97	4.04	2.05	γH 0.96, 1.07	N119	117.7	8.13	5.13		
E52	126.8	8.22	4.43			T120	124.2	10.68	3.86	3.81	γH 0.77
K53	125.6	8.58	3.80			H121	113.2	6.82	5.43		
Y54	115.8	8.64	4.42	3.10, 3.38	δH 6.79; εH 6.72	E122					
G55	108.4	8.83	3.71, 3.72			Q123			4.20[b]		
P56						H124	120.1	8.15	4.38		
E57						L125	118.2	8.08	3.95		
A58	124.2	8.88	4.17	1.73		R126	118.6	8.90	4.02		
S59	111.7	8.29	3.72			K127	122.3	7.98	4.13		
A60	122.3	8.38	4.06	1.52		S128	118.0	7.58	4.27		
F61	121.4	8.08	4.04	3.10, 3.35	δH 7.12; εH 7.22; ζH 7.19	E129	125.1	8.44	3.87		
T62	120.3	8.60	3.59	4.11	γH 1.03	A130	119.6	7.94	3.84	1.49	
K63	120.1	8.12	3.59			Q131	118.3	7.42	3.98		
K64	117.3	7.92	3.95			A132	123.0	7.85	3.95	1.76	
M65	116.3	7.64	3.92			K133	117.2	8.14	3.45		
V66	107.8	8.28	4.15	2.17	γH 0.89, 1.15	K134	122.3	7.76	3.97		
E67	121.2	8.77	3.97			E135	116.6	7.62	4.04		
N68	113.4	7.33	4.68			K136	116.6	7.80	3.56		
A69	121.3	6.69	4.54	1.35		L137	117.1	7.57	4.18		
K70	125.6	10.12	4.36			N138	118.6	9.04	3.79		
K71	121.4	8.87	4.65			I139	124.4	8.33	3.32		
I72	129.1	8.92	5.22			W140	119.2	7.83	4.92	2.82, 3.69	H1 11.59; H2 6.96; H4 7.65; H5 7.04; H6 7.11; H7 7.52
E73	123.3	8.80	5.27								
V74	117.2	9.53	4.61	1.30	γH −0.12, 0.33						
E75	126.8	8.84	5.17			S141	116.2	8.09	4.20		

[a] Chemical shifts are in ppm referenced to liquid ammonia, ^{15}N, and TSP, ^{1}H. Uncertainties are ±0.1 ppm, ^{15}N, and ±0.02 ppm, ^{1}H. Values are for Nase at 37 °C, pH 7.4 ± 0.1. [b] From Bax et al. (1988b). [c] Split peak.

[^{15}N]Thr HMQC spectrum, Figure 1Sc, and the PS COSY spectrum, Figure 6. The NH–α correlations of (a) T22 and T82 follow from the unique α-shifts of these residues and of (b) T41 and T120 follow from the unique NH shifts of these residues, Figure 9. The T62 spin system identification is based upon the observation of NH–α, NH–β, and NH–γ cross-peaks

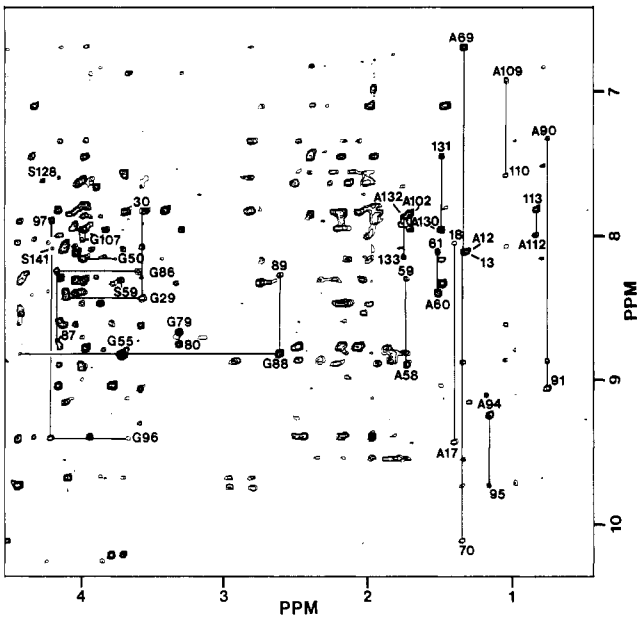

FIGURE 5: Amide–aliphatic connectivities in the 500-MHz NOESY spectrum of deuteriated Nase. The Ala $d_{N\beta}(i,i)$ connectivities are identified and linked to the sequential $d_{\beta N}$ connectivities by solid lines. In the downfield aliphatic region, Ser and Gly $d_{N\alpha}$ connectivities are identified, and several of the intraresidue Gly connectivities are linked to sequential $d_{\alpha N}$ connectivities by solid lines. When two Gly $d_{N\alpha}(i,i)$ connectivities are identified, they are joined by dashed lines. Note that all sequential connectivities $(i,i+1)$ are identified by the single number $i + 1$. Spectrum recorded with water presaturation, pH 7.0.

in the NOESY spectrum, Figure 8. The α-proton of T33 is identified in the HMBC (Westler et al., 1988; Bax et al., 1988) spectrum of Nase labeled with [^{15}N]Phe/[1-^{13}C]Thr, and the T33 NH is assigned in the HMQC spectrum of Nase labeled with [1-^{13}C]Met/[^{15}N]Thr, Figure 1Sc. The amide protons of T13 and three other residues resonate in the 8.10–8.14 ppm range, Figure 9. Although all four amide protons exhibit NH–α connectivities in the PS COSY spectrum, Figure 6, only the connectivity at 8.12, 4.72 ppm matches an available Thr α-proton shift and is therefore assigned to T13. The NH–α connectivity of T44 has not been identified.

The Val spin systems are identified in the HOHAHA spectrum of deuteriated Nase containing protiated Val, Figure 10a, which shows β–γ correlations for all 10 Val spin systems and α–γ correlations for all Val residues except V39 and V66. The shifts of the Val NH protons are known from previous work (Torchia et al., 1988b). The Val NH–aliphatic proton connectivities are clearly observed in the regular NOESY spectrum, Figure 8, for V99 because its NH chemical shift, 10.20 ppm, is unique. Equally clear Val NH–aliphatic correlations are seen for the remaining Val residues in the edited NOESY spectrum of Nase labeled with [^{15}N]Val. Only the V5′ protons, which we assign to the N-terminus of Nase because of their large T_2 values and random coil shifts, fail to show NOESY connectivities in Figure 10b. The Val39 and -66 connectivities identified in Figure 10b are confirmed by the ^{15}N–NH–α J-correlations identified in Figure 13. These connectivities are unambiguous because the only residues having the same ^{15}N shifts as V39 and V66 are G20 and T82, respectively, and their α-protons have been identified.

Identification of Phe, Tyr, and Trp Spin Systems. The unique connectivity patterns of the Phe, Tyr, and Trp ring spin systems (Wuethrich, 1986) in the aromatic region of the HOHAHA spectrum, Figure 11a, lead to the immediate identification of the J-coupled Phe, Tyr, and Trp ring protons. The identification of the complete Trp140 spin system is based on the following analysis. The Trp H4 proton at 7.65 ppm shows strong NOESY correlations to α- and β-protons at 4.92, 3.69, and 2.82 ppm, respectively, Figure 11b; furthermore, the Trp α-proton shows a strong HOHAHA correlation to the β-proton at 3.69 ppm, which is in turn correlated to the other Trp β-proton, Figure 4. The Trp α- and β-protons show strong NOESY correlations to the Trp H2 proton at 6.96 ppm, and the Trp H2 and H7 protons show strong NOESY correlations to the H1 proton at 11.59 ppm, Figure 3S. As expected, these correlations are absent in the NOESY spectrum of deuteriated Nase, which contains [ring-$^2H_5$]Trp. The connectivities of the Trp α- and β-protons with the Trp H2 and H4 protons are observed in the natural abundance NOESY spectrum, Figure 8, as are connectivities of the Trp α- and β-protons with the Trp amide proton at 7.82 ppm. This amide proton assignment is strongly confirmed by the observation of strong NH–α, NH–β_1, and NH–β_2 NOE connectivities in the NOESY spectrum of deuteriated Nase, Figure 4S, a sample containing Trp deuteriated on the ring but protiated at the α- and β-carbons. The Trp amide proton and α-proton assignments are reinforced by the Trp NH–α connectivity observed in the PS COSY spectrum, Figure 6.

The δ- and ϵ-proton signals of the eight Tyr residues are identified by combining the chemical shifts derived from the HOHAHA connectivities, Figure 11a, with chemical shifts derived from one-dimensional proton spectra of Nase labeled with either [ring-$^2H_5$]Phe and [δ,δ-$^2H_2$]Tyr or [ring-$^2H_5$]Phe and [ϵ,ϵ-$^2H_2$]Tyr (Hibler et al., 1987). The Tyr β-protons are identified in the HMQC spectrum of Nase labeled with [3-^{13}C]Tyr, Figure 3b, and strong β–δ NOE connectivities are found for all Tyr residues except Y6′ and Y91, Figure 11b. The absence of β–δ NOE cross-peaks in the case of Y91 is a consequence of the broad δ-proton signals observed for Y91, Figure 11a. With the exception of Y91, α–β HOHAHA connectivities are observed for all Tyr residues, Figure 4, and with the exceptions of Y27 and Y133 whose β–β cross-peaks fall in a crowded region near the diagonal of the HOHAHA spectrum, all Tyr β–β HOHAHA connectivities are observed. The eight Tyr NH signals, identified in the HMQC spectrum, Figure 1Sd, of Nase labeled with [^{15}N]Tyr are correlated to the Tyr β-protons by means of N–β NOESY connectivities, Figure 8, observed for all Tyr residues except Tyr6′. Because the Tyr6′ protons exhibit no NOE connectivities and have random coil chemical shifts and large T_2 values, they are assigned to the one Tyr residue in the N-terminal region of Nase. Finally, we note that many Tyr α–δ, β–δ, and β–ϵ NOE connectivities can be identified in Figure 8, and all Tyr N–α connectivities not obscured by the water signal are observed in the PS COSY spectrum, Figure 6.

The three Phe β-protons are identified in the HMQC spectrum of Nase labeled with [3-^{13}C]Phe. The β-protons are correlated to the Phe α-protons by a HMQC/RELAY spectrum of this sample and by Phe α–β HOHAHA connectivities, Figure 4. The Phe α- and β-protons are correlated to the Phe δ-protons, identified in the HOHAHA spectrum, Figure 11a, by strong α–δ and β–δ NOE connectivities, Figure 11b. The Phe NH protons previously identified (Torchia et al., 1988b) are correlated to the Phe β-protons by strong N–β NOE connectivities, Figure 8. Phe α–δ, β–δ, and β–ϵ connectivities can also be identified in this spectrum. We also note that the three Phe NH–α connectivities are observed in the PS COSY spectrum, Figure 6.

Sequential Assignments of Residues in the Long Sequences of d_{NN} Connectivities. The NH protons in three long d_{NN} connectivity sequences, identified as 1, 2, and 3 in Figure 14,

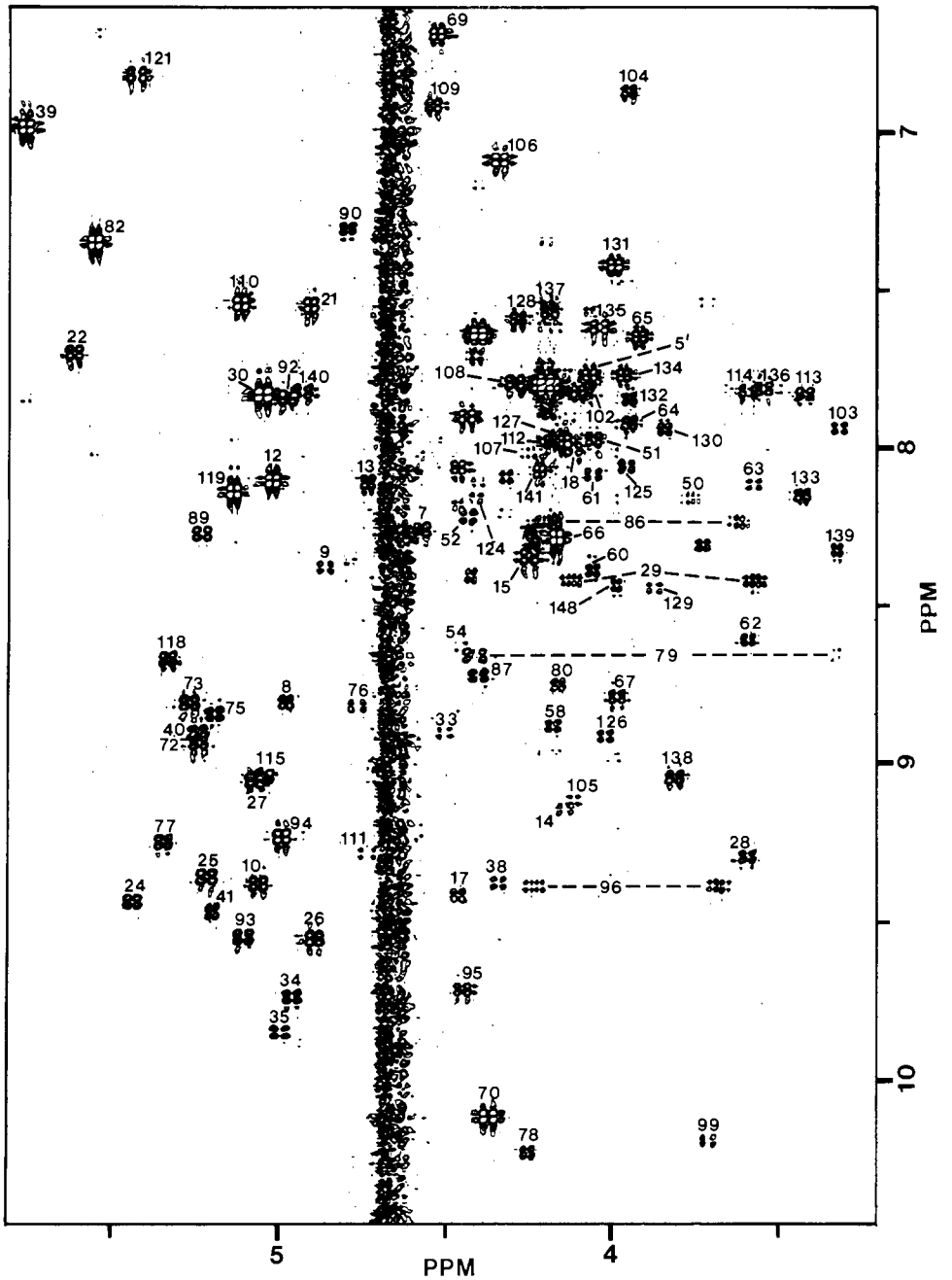

FIGURE 6: 600-MHz PS COSY spectrum of ^{15}N-labeled Nase in the fingerprint region, pH 6.5.

have been assigned by Torchia et al. (1988b). For completeness, these assignments are included in Table III. The chemical shifts listed in Table III were obtained from the NOESY spectrum of protiated Nase, Figure 12, and are all within 0.02 ppm of the NH chemical shifts reported for deuteriated Nase (Torchia et al., 1988b). The one exception to this statement is the NH of K63 whose chemical shift in Table III is 0.06 ppm larger than that reported in deuteriated Nase.

Assignments of the α-Protons of Residues 58–69. The known NH assignments together with the spin system identifications given above provide α-proton assignments of residues 58–62, 66, and 69. The α-proton assignments of M65, V66 (already assigned), and E67 follow directly from the ^{15}N–NH–α correlations, Figure 13, because these residues have unique connectivities in the HMQC spectrum of Nase uniformly labeled with ^{15}N, Figure 9. The α-proton of K63 is assigned by virtue of NOESY connectivities with the NH protons of K63, K64, and V66 observed in edited NOESY spectra, Figures 7c and 10b. The α-proton of F61 also shows a connectivity to the NH of K64, Figure 7c, and the remaining connectivity involving K64 is assigned to K64 NH–α. The α-proton of N68 has not been identified, suggesting that it may coincide with the water signal. With the exception of N68, the N–α connectivities of all residues in the 58–69 region of the sequence are also identified in the PS COSY spectrum, Figure 6.

Assignments of the α-Protons of Residues 99–109. The NH assignments and spin system identifications provide assignments of α-protons of residues V99, A102, V104, G107, and A109. The α-protons of E101, Q106, and L108 follow from ^{15}N–NH–α correlations, Figure 13. The N100 α-proton is assigned on the basis of its connectivities to the isolated NH protons of N100 and E101 in the NOESY spectrum, Figure 8, and the NOESY spectrum of deuteriated Nase, Figure 4S. The L103 NH shows an N–α NOESY correlation to the nearly degenerate α-protons of A102 and N100 in Figure 7b; the remaining correlation is assigned to L103 N–α. Because

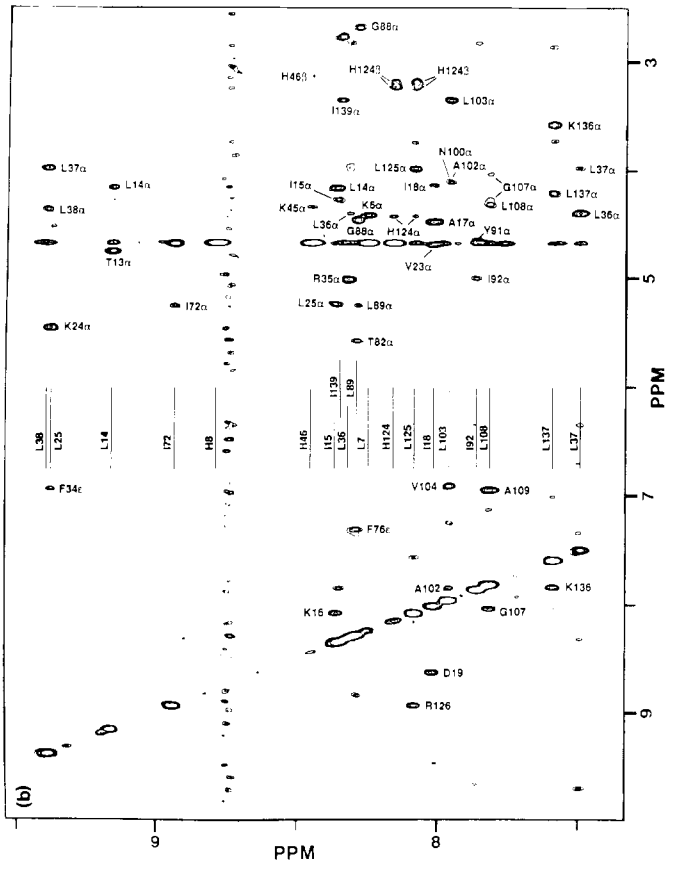

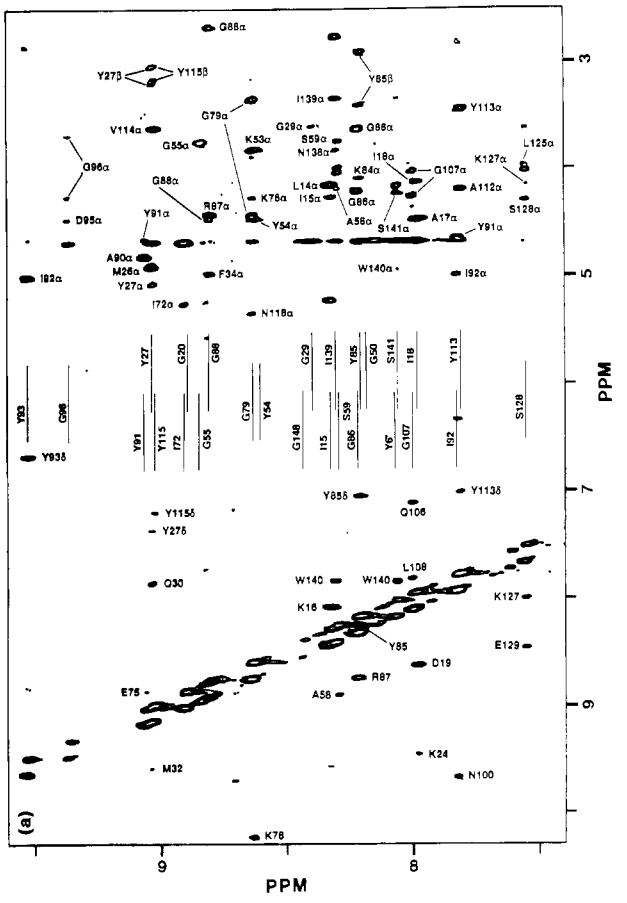

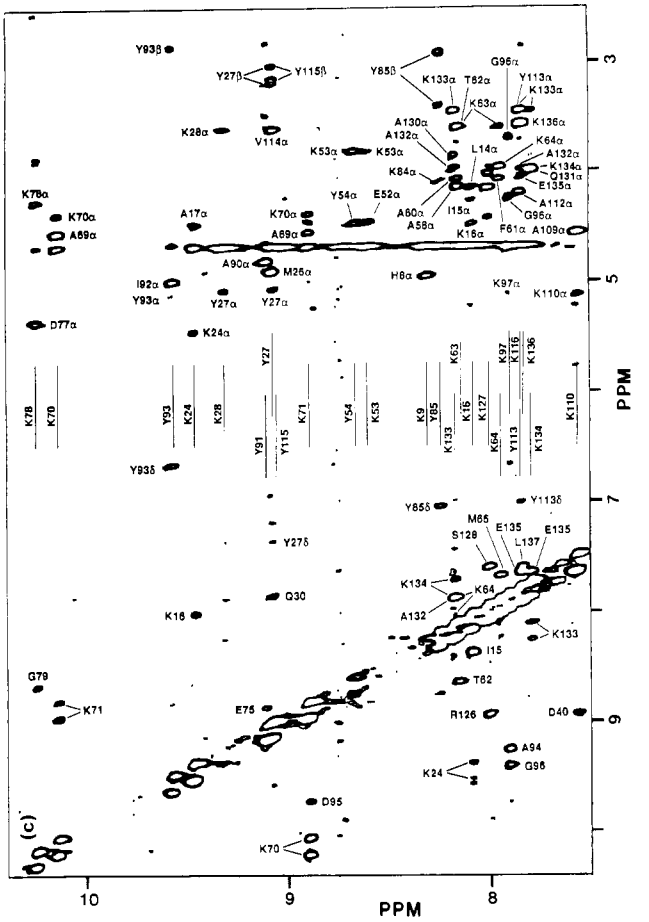

FIGURE 7: 600-MHz ^{15}N-edited NOESY spectra of Nase labeled with (a) [^{15}N]G/[^{15}N]I/[^{15}N]S/[^{15}N]Y, (b) [^{15}N]H/[^{15}N]I/[^{15}N]L, and (c) [^{15}N]K/[^{15}N]Y. Mixing time, 110 ms; pH 7.4. Amide–amide, amide–aromatic, and amide–aliphatic connectivities are labeled. The latter are not labeled for K127 in panel c because of lack of space.

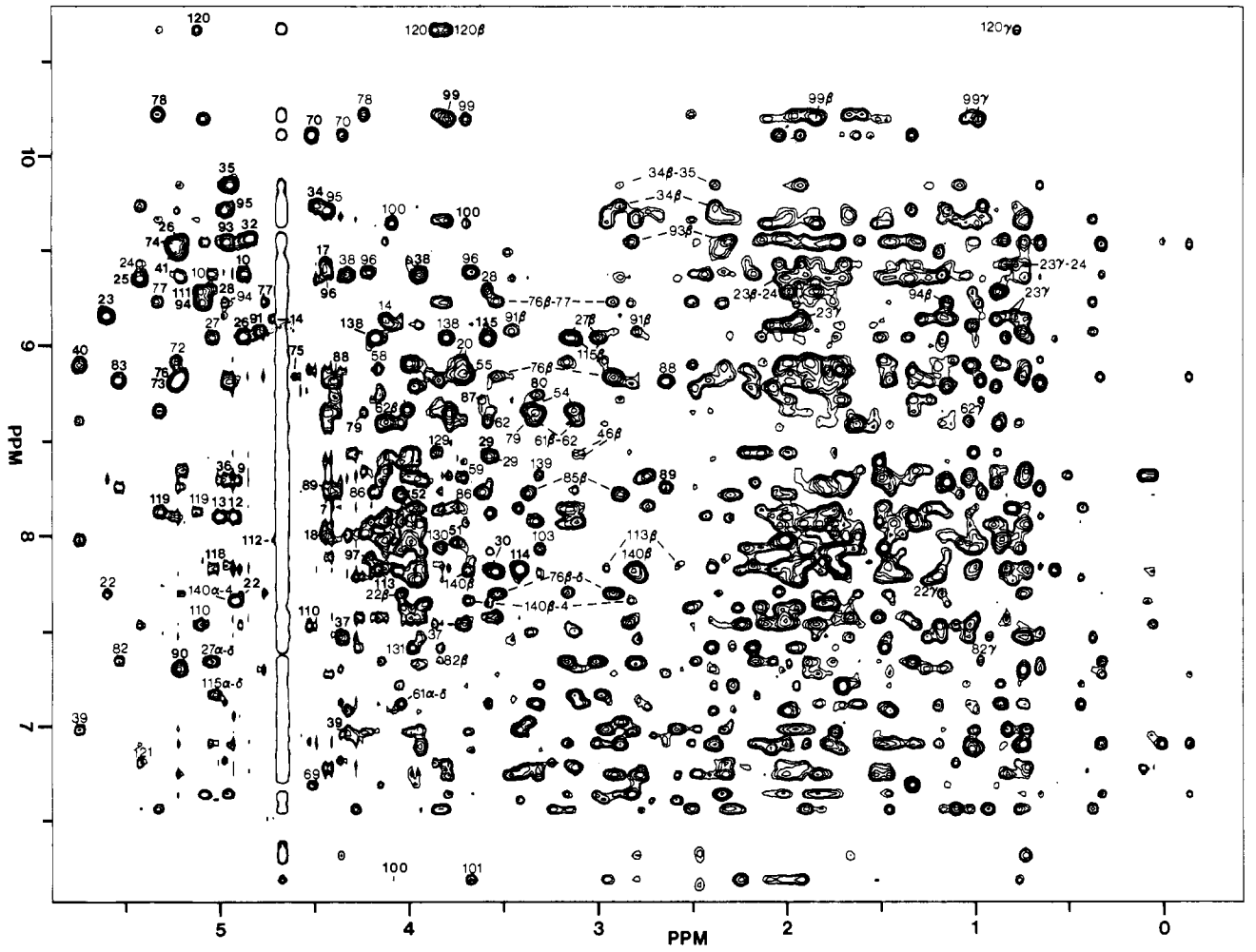

FIGURE 8: Amide–aliphatic and aromatic–aliphatic connectivities in the 600-MHz NOESY spectrum of Nase: mixing time, 100 ms; pH 7.4. No presaturation and a 1–1 read pulse at the end of the mixing period were used. Connectivities $d_{N\alpha}(i,i)$ and $d_{\alpha N}(i,i+1)$ are labeled with numbers i and $i+1$, respectively, the latter in boldface to distinguish them from the former. Intraresidue N–β and N–γ connectivities are indicated by the residue number followed by the appropriate Greek letter. Intraresidue aromatic connectivities are indicated by the residue number and the Greek letters of the protons involved. Note that numbers are used to identify the Trp ring protons. $d_{\beta N}(i,i+1)$ connectivities are labeled $i\beta,i+1$.

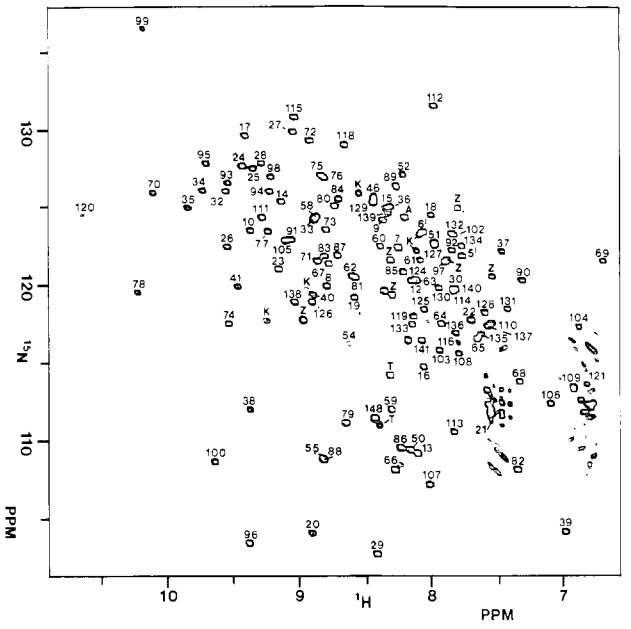

FIGURE 9: ^1H–^{15}N HMQC spectrum of ^{15}N-labeled Nase, pH 6.5. This spectrum, obtained with a 1–1 echo sequence (Roy & Redfield, 1984; Sklenar & Bax, 1987), can be compared with the spectrum of the same sample acquired with water saturation, Figure 6S.

the NH proton of R105 has a unique chemical shift at 9.12 ppm, Figure 9, its α-proton is assigned by means of the Arg105 N–α connectivity observed in the PS COSY spectrum, Figure 6. With the exception of N100, all N–α connectivities of residues 99–109 are observed in the PS COSY spectrum.

Assignments of the α-Protons of Residues 124–137. The NH assignments and spin system identifications provide the assignments of α-protons of S128, A130, and A132. HMQC spectra of [1-^{13}C]Thr/[^{15}N]His-labeled (Torchia et al., 1988b) and [1-^{13}C]Leu/[^{15}N]His-labeled, Figure 2b, Nase show that the shift of H124 NH is either 8.44 or 8.15 ppm. The latter value is assigned to H124 because this NH has d_{NN} connectivities with the L125NH in the edited NOESY spectrum of Nase labeled with [^{15}N]His and [^{15}N]Leu, Figure 7b. Both the L125 and H124 NH protons also have NOE connectivities with the H124 α- and β-protons. The remaining strong L125 NH–α connectivity is assigned to the Leu125 intraresidue NH–α NOE. This assignment is confirmed by the S128NH–L125α connectivity observed in the edited NOESY spectrum of Nase labeled with [^{15}N]Ser, Figure 7a. This spectrum also shows a weak S128NH–K127α connectivity whose assignment is reinforced by the strong K127 NH–α connectivity seen in Figure 7c. The K127NH also shows a connectivity with an α-proton at 4.02 ppm, assigned to R126. The NH proton of

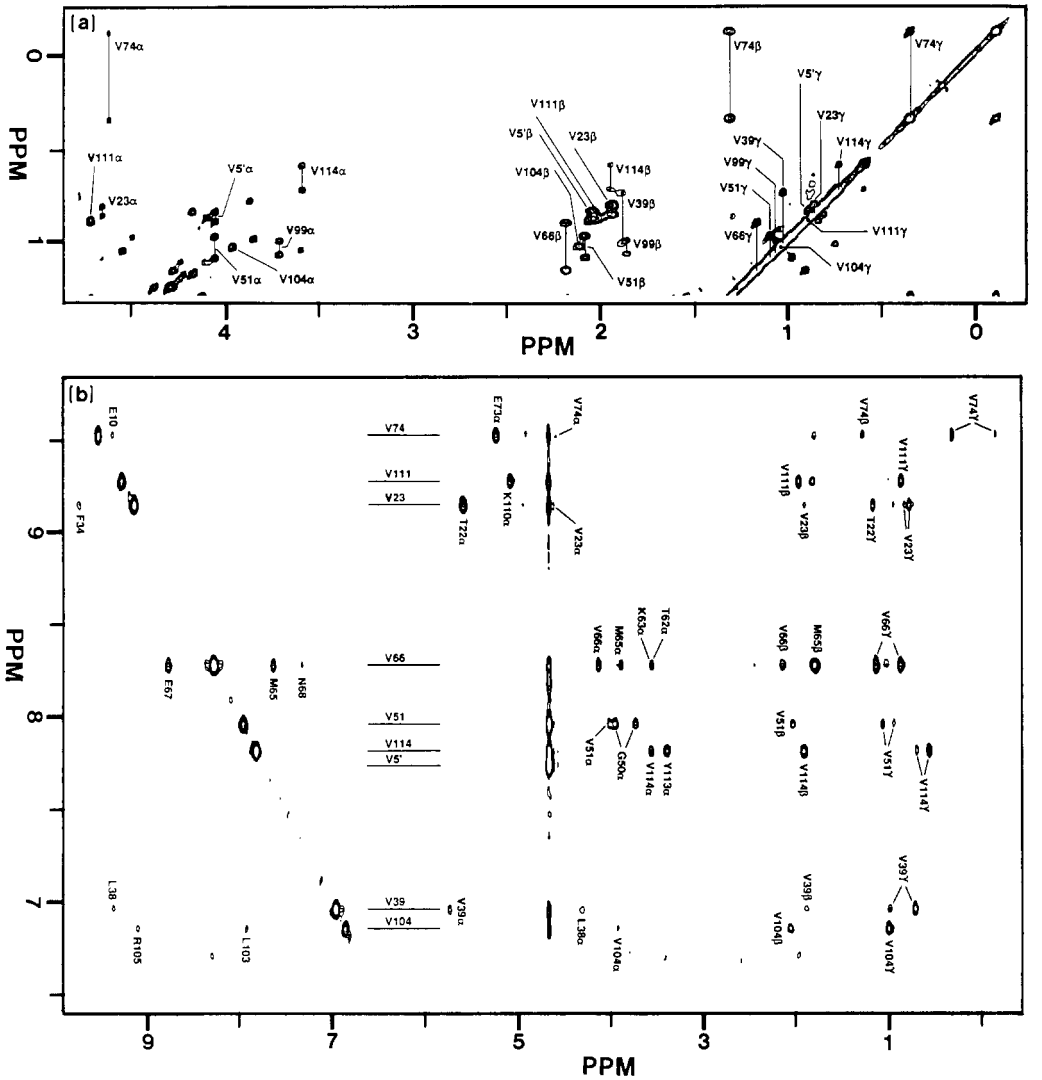

FIGURE 10: (a) 500-MHz HOHAHA spectrum of deuteriated Nase containing protiated Val and Met. Val α–γ, β–γ, and γ–γ connectivities are labeled. Mixing time, 60 ms. (b) 600-MHz ^{15}N-edited NOESY spectrum of Nase labeled with [^{15}N]Val: mixing time, 100 ms; pH 7.4. Connectivities involving Val amide protons are identified.

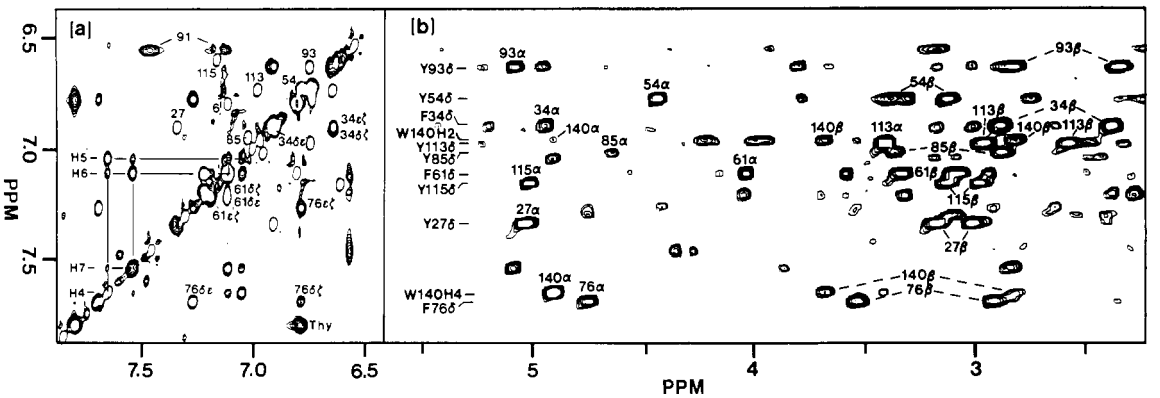

FIGURE 11: (a) Aromatic region of the 600-MHz HOHAHA spectrum of Nase exchanged with ^2H_2O: mixing time, 35 ms; pH 7.4. The Tyr δ–ϵ connectivities are identified by residue number, and the connectivity-labeled Thy is an exchange cross-peak involving the H6 protons of free and bound pdTp. Note that the Trp140 ring protons are identified by number. (b) Aromatic–aliphatic region of the 500-MHz NOESY spectrum of Nase labeled with [ϵ,ϵ-$^2H_2$]Tyr: mixing time, 150 ms. The connectivities involving the ring protons and aliphatic protons of the aromatic residues are labeled.

K133 shows three N–α NOE connectivities; two connectivities are with the assigned α-protons of A130 and A132, Figure 7c, and a third connectivity is with an α-proton at 3.45 ppm assigned to K133. This assignment is confirmed by the K133α–K136NH connectivity observed in Figure 7c. K136NH shows connectivities with K136α and E135α. The latter assignment is confirmed by the strong E135 NH–α connectivity observed in the NOESY spectrum of deuteriated Nase, Figure 4S. In addition to Ala residues, Asx and Glx residues show relatively high levels of protiation at α- and β-carbons in the deuteriated Nase sample, and N–α NOE connectivities are observed for E129 and Q131, Figure 4S.

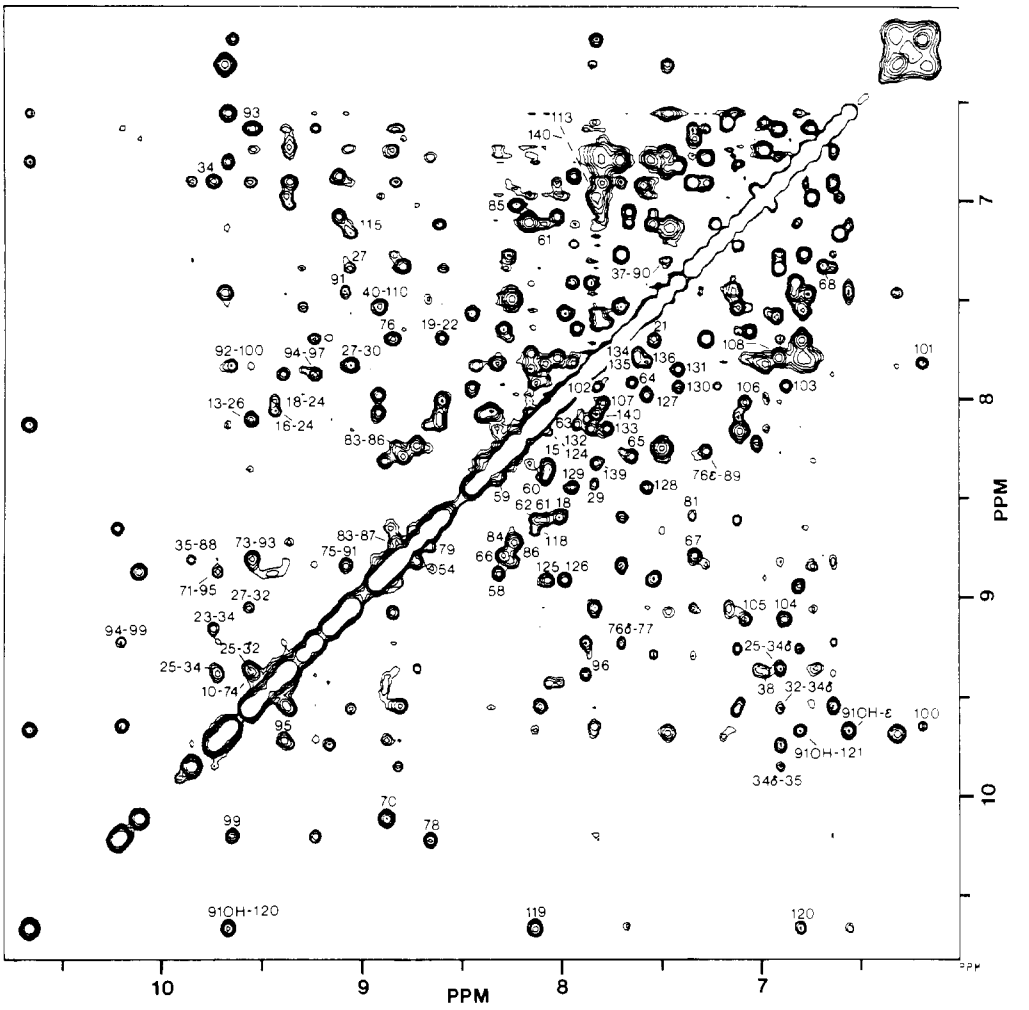

FIGURE 12: NH and aromatic region of the 600-MHz NOESY spectrum of Nase: mixing time, 100 ms; a 1–1 read sequence without water presaturation; pH 7.4. Sequential connectivities $d_{NN}(i,i+1)$ are labeled below the diagonal with the residue number i, along with long-range connectivities involving aromatic ring protons and NH protons. Long-range d_{NN} connectivities and intraresidue aromatic NH–δ connectivities are labeled above the diagonal.

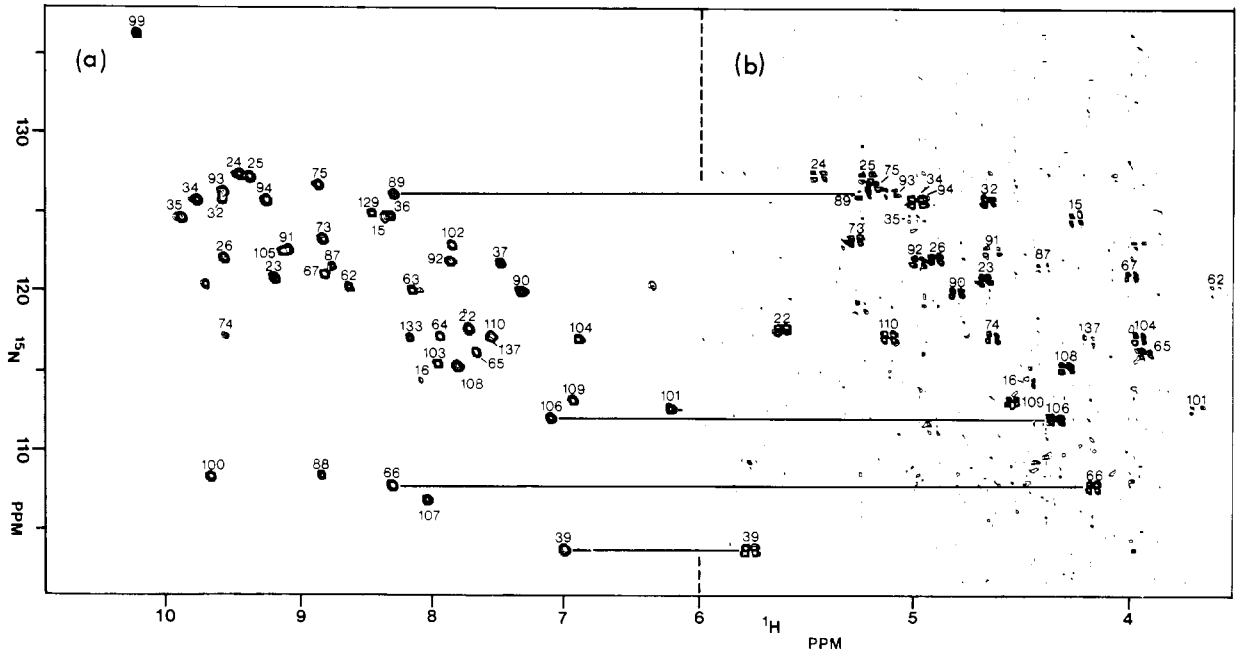

FIGURE 13: (a) ^{1}H–^{15}N 500-MHz HMQC spectrum of ^{15}N-labeled Nase after the sample had exchanged with $^{2}H_2O$ for ca. 24 h at 37 °C. (b) ^{1}H–^{15}N HMQC–COSY spectrum, see Figure 1c for pulse sequence, of the same sample. Because of their common ^{15}N shifts, the ^{15}N–NH and ^{15}N–α connectivities within one residue were readily linked by straight lines as illustrated in the figure. Note that not every ^{15}N–NH connectivity has a corresponding ^{15}N–α connectivity because the latter are too weak to detect when proton J-couplings are small. pH 6.5.

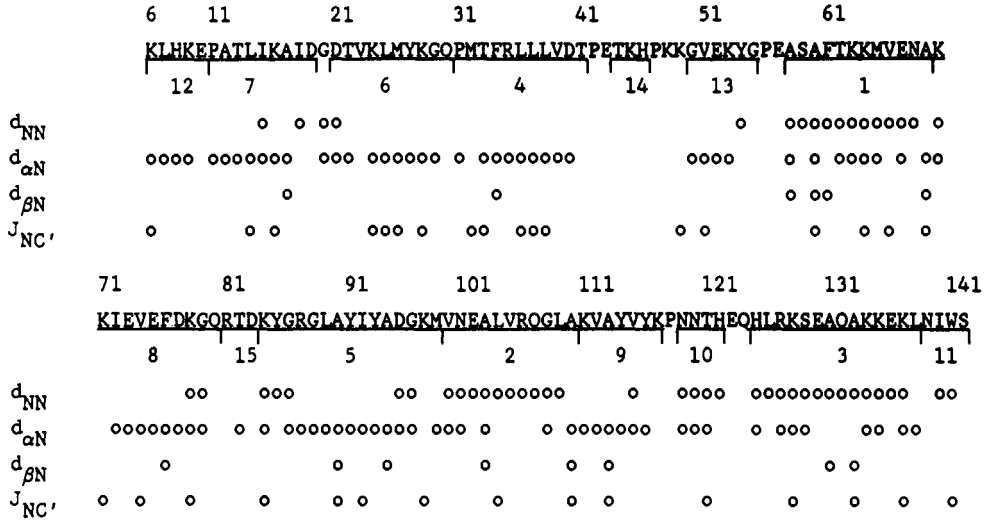

FIGURE 14: Amino acid sequence of the structured region of Nase, summary of sequential connectivities, and 1-^{13}C/^{15}N sequential couplings, $J_{NC'}$, used in the assignment procedure. Numbers under the peptide segments indicate the order in which segments were assigned.

Returning to Figure 7c, we note that K134NH shows a single strong connectivity at 3.98 ppm, suggesting that the α-proton shifts of Q131 (just assigned) and K134 are ca. equal to 4.0 ppm, an assignment that is confirmed by the K134 N–α connectivity observed in the PS COSY spectrum, Figure 6. Figure 7b shows that the L137NH has a strong connectivity to the α-proton of K136 and a second strong connectivity to its own α-proton. This latter assignment is confirmed by the L137 ^{15}N–NH–α connectivity, Figure 13. All α-protons assigned to residues 124–137 are confirmed by NH–α connectivities observed in Figure 6.

Assignments of Residues 31–41. Sequential assignments of all three Phe spin systems follow from the Phe NH sequential assignments (Torchia et al., 1988b) and the Phe spin system identifications provided herein. The F34 NH–α correlation observed in the edited NOESY spectrum of [^{15}N]-Phe-labeled Nase, Figure 5Sa, is assigned to T33α–F34NH because the α-proton shift matches that of a Thr residue. A M32α–T33NH correlation is not observed in the edited NOESY spectrum of Nase labeled with [^{15}N]Thr, because as seen in Figure 13 the M32 α shift coincides with the water signal. (The assignment of the M32 α-proton is unambiguous because the α-protons of F34 and A94 have been identified.) The P31α–M32NH correlation, identified in the edited NOESY spectrum of Nase labeled with [^{15}N]Met, Figure 5Sb, is supported by the observation of a proline α-proton at 4.84 ppm in the HMQC spectrum, Figure 2Sd, of Nase labeled with [2-^{13}C]Pro. The unique amide proton at 9.85 ppm, Figure 9, is assigned to R35 because it has NOESY connectivities to the α-, β-, and δ-protons of F34, Figures 8 and 12. The PS COSY spectrum, Figure 6, provides the assignment of the R35 α-proton which is linked to the NH of L36 in Figure 7b. Previous Leu NH assignments, together with Leu NH type assignments derived from Figure 2b, require that the L36NH shift equal 8.26, 8.30, or 9.14 ppm. As only the Leu NH at 8.30 ppm shows a connectivity with R35 α, Figure 7b, this connectivity is assigned to R35α–L36NH and is the starting point of a sequence of $d_{\alpha N}$ and $d_{N\alpha}(i,i)$ connectivities that link residues 35–38, Figure 7b. The NH assignments of L37 and L38 provided by Figure 7b are confirmed by the observation that the connectivities of these residues are doublets in the HMQC spectrum of Nase labeled with [1-^{13}C,^{15}N]Leu, Figure 2b. $d_{\alpha N}(38,39)$ and $d_{N\alpha}(39,39)$ connectivities are identified in Figure 10b. The shift of V39α, 5.75 ppm, is unique, and the intense $d_{\alpha N}$ connectivity involving this proton, Figure 8, is assigned to V39α–D40NH. Inspection of Figures 6 and 9 shows that the shift of D40α must be 5.21 ppm, and the connectivity involving this proton in the edited NOESY spectrum of [^{15}N]Thr-labeled Nase, Figure 5Sc, is assigned to D40α–T41NH. The T41α assignment follows from the Thr spin system identifications. We note that all $d_{\alpha N}$ connectivities observed in the edited NOESY spectra are also identified in Figure 8.

Assignments of Residues 84–98. The doublet in the HMQC spectrum of Nase labeled with [1-^{13}C]Ile/[^{15}N]Tyr, Figure 2Sd, provides the assignment of Y93NH, and the Y93α assignment follows from the Tyr spin system identifications. The N–α connectivities, identified in the edited NOESY spectrum of Nase labeled with [^{15}N]I and [^{15}N]Y, Figure 7a, yields NH and α assignments for I92 and Y91 and the α assignment of A90. The A90NH assignment follows from the Ala spin system identifications. Figure 8 shows a very intense NOE between A90 and an α-proton at 5.22 ppm. This α-proton has a connectivity with a Leu NH at 8.27 ppm, Figure 7b, which we identify as the Leu89 N–α connectivity because 8.27 ppm is one of only two possible NH shifts that remain available to L89. Two G88α–L89NH and two G88 NH–α connectivities are observed in panels a and b of Figure 7, respectively. The latter figure also shows a correlation from G88NH to a proton at 4.40 ppm assigned to R87α. Figures 5, 9, and 13 show that an α-proton at 4.40 ppm correlates with the unique NH at 8.87, which is assigned to R87. This assignment is confirmed by the observation of R87NH–G86NH and R87NH–G86α connectivities in Figures 7a and 8, respectively. The d_{NN} and $d_{\alpha N}$ connectivities involving G86 and Y85, identified in Figure 7a, are confirmed by the HMQC spectrum of Nase labeled with [1-^{13}C]K/[^{15}N]Y, Figure 1Sb, which shows that the ^{15}N–NH correlation assigned to Y85 is a doublet. The Y85α shift is coincident with the water signal, Figure 4, making the Y85 N–α correlation unobservable in Figure 7a. Therefore, Y85NH exhibits a NOE correlation to only one α-proton, assigned to K84 in Figure 7a.

The Ala NH with the unique shift of 9.22 ppm shows NOE connectivities to its α- and β-protons, Figures 5 and 8. It also has connectivities to the α- and β-protons of Y93 and is therefore assigned to A94NH. Figures 5 and 8 show A94β–D95NH connectivities, and the D95 N–α connectivity is readily identified in Figure 6 because the D95NH shift is unique, Figure 9. NOE connectivities linking D95NH to its α-proton as well as to the two α-protons of G96 are identified

in Figures 7a and 8. G96 N–α connectivities are also seen in these figures. The K97NH–G96α and K97 NH–α connectivities are identified in Figure 7c. the K97α–M98NH connectivity has not been found, most likely because the M98NH is exchange broadened (Torchia et al., 1988b). The M98α–V99NH connectivity is identified in Figure 8.

Assignments of Residues 21–30. The T22α–V23NH connectivity is readily identified in Figure 10b because the Thr22 α-shift is unique and Nase contains one Thr–Val peptide bond. Because the shift of V23α coincides with that of water, we approach the assignment of K24 from M26. The previous identification of the M26 ^{1}H–^{15}N connectivity in the HMQC spectrum (Torchia et al., 1988b) and Figure 13 provide the M26α assignment, and the L25α–M26NH connectivity seen in the edited NOESY spectrum, Figure 5Sb, of Nase labeled with [^{15}N]Met yields the L25α assignment. It has been shown (Torchia et al., 1988b) that the NH of L25 must occur at either 8.24 or 9.37 ppm, and Figures 6 and 13 show connectivities only between the L25 α-proton and an NH at 9.37 ppm. The strong K24α–L25NH connectivity identified in Figure 7b puts the K24α at 5.43 ppm. Of the two possible PS COSY connectivities at 5.43 ppm only the one assigned to K24 has an NH shift that matches a Lys NH shift observed in the HMQC spectrum of Nase labeled with [^{15}N]Lys, Figure 1Se. The K24 assignment is confirmed by NOE connectivities seen between the K24NH and the β- and γ-protons of Val23, Figure 8.

The NH of Y27 is assigned in the HMQC spectrum of Nase labeled with [1-^{13}C]Met/[^{15}N]Y, Figure 2Sc. This amide proton has correlations to its α- and β-protons and to the M26 α-proton, Figure 7a. The NH assigned to K28 shows correlations to the α-protons of Y27 and K28 in Figure 7c. The NH of G29 shows correlations to the K28 and G29 α-protons, Figure 7a and 8, while the G29 α-protons show correlations to the G29 and Q30 NH protons, Figures 5 and 8. The ^{15}N–NH correlation assigned to G29 is a doublet in the HMQC spectrum of Nase labeled with [1-^{13}C]K/[^{15}N]G, Figure 2Sb. Finally, we assign the NH of D21 on the basis of the d_{NN}(21,22) connectivity identified in Figure 12 and the D21 ^{15}N–NH connectivity identified in the HMQC spectrum of Nase labeled with [^{15}N]Asx, Figure 1Sa.

Assignments of Residues 11–19. The NH of I15 is assigned on the basis of the HMQC spectrum of Nase labeled with [1-^{13}C]L/[^{15}N]I, Figure 2b, and the NH of L14 is assigned to 9.14 ppm by elimination, because all other Leu NH shifts have been identified. The $d_{N\alpha}(i,i)$ and $d_{\alpha N}$ connectivities of I15, L14, and T13 are identified in Figure 7b. The assignment of the T13NH follows from the T13α assignment and the Thr spin system identifications, and the A12α assignment follows from the A12α–T13NH connectivity seen in the edited NOESY spectrum of Nase labeled with [^{15}N]Thr, Figure 5Sc, and the A12NH is then assigned by the spin system identifications. The strong $d_{\alpha N}$ connectivity at 4.93, 8.11 ppm, Figure 8, is assigned to $d_{\alpha N}$(11,12) because its chemical shifts match those of a proline α-proton, Figure 2Sd, and the A12 NH proton.

A strong d_{NN} cross-peak involving I15 is observed in Figure 7b, at 8.34, 8.06 ppm, and the Lys NH at 8.06 ppm shows a reciprocal cross-peak with the NH at 8.34 ppm, Figure 7c, which is assigned to the K16NH because I15 is the only Ile adjacent to a Lys residue. The K16NH connectivities to the I15 and K16 α-protons are seen in Figure 7c. The NH of A17 is assigned from the HMQC spectrum of Nase labeled with [1-^{13}C]K/[^{15}N]A, Figure 2a, and the A17α shift follows from the Ala spin system identifications. The $d_{\alpha N}$(16,17) connectivity is identified in Figure 8. The I18NH is assigned on the basis of its connectivities to the α- and β-protons of A17, Figures 7b and 5. The I18 N–α connectivity is also seen in the former figure. The strong d_{NN} connectivity involving I18 and an amide at 8.63 ppm, Figure 12, is assigned to I18–D19, because an NH is observed at 8.63 ppm in the HMQC spectrum of Nase labeled with [^{15}N]Asx, Figure 1Sa.

Assignments of Residues 70–80. The broad asymmetric signals of K70, K110, and K133 are identified in the HMQC spectrum of Nase labeled with [1-^{13}C]A/[^{15}N]K, Figure 1Se. Because K133 is assigned, the K70 NH proton is assigned to 10.12 ppm on the basis of the A69β–K70NH connectivity seen in Figure 5. By elimination, K110NH is assigned to 7.54 ppm. The K70α assignment follows from the PS COSY spectrum, and the K71α assignment follows from the d_{NN}, $d_{\alpha N}$, and $d_{N\alpha}(i,i)$ connectivities observed in Figure 7c. The NH of I72 is identified in the HMQC spectrum of [1-^{13}C]K/[^{15}N]I, Figure 1Sb, and its α-proton shift is obtained from the PS COSY spectrum, Figure 6, because the I72 NH shift is unique, Figure 9. The only remaining unassigned NH–α connectivity, involving an α-proton at 5.22 ppm in Figure 8, is with an amide NH at 8.80 ppm which matches a Glx chemical shift seen in the HMQC spectrum, Figure 1Sa, of [^{15}N]Glx-labeled Nase and is therefore assigned to I72α–E73NH. The E73α shift is obtained from Figure 13, and this proton shows a strong connectivity to the Val74 NH in Figures 10b and 8. The V74α assignment follows from the spin system identifications and is verified in Figure 13. Although the V74α shift resonates close to water, it has weak connectivity to an NH at 8.84 ppm, Figure 8, and an NH with this shift is a doublet in the HMQC spectrum of Nase labeled with [1-^{13}C]V/[^{15}N]Glx, not shown, and is therefore assigned to E75. The E75α assignment follows from Figures 6 and 13. Strong E75α–F76NH connectivities are seen in Figure 8 and in the edited NOESY spectrum of Nase labeled with [^{15}N]Phe, Figure 5Sa.

Residues 77–80 are assigned by the series of sequential connectivities identified in Figure 8. These assignments are confirmed by (a) connectivities in the PS COSY spectrum, (b) $d_{N\alpha}(i,i)$ and $d_{\alpha N}$ connectivities in edited NOESY spectra, Figure 7a,c (c) the K78-G79-E80 d_{NN} connectivities identified in Figures 7c and 12, (d) the fact that the NH assignments of K78, G79, and E80 are consistent with NH-type assignments derived from the ^{1}H–^{15}N HMQC spectra, (e) the observation of a G79NH doublet in the HMQC spectrum of Nase labeled with [1-^{13}C]K/[^{15}N]G, Figure 1Sb, and (f) the identification of the N77NH in the HMQC spectrum of Nase labeled with [^{15}N]Asx. Finally, the N77 α- and β-protons assigned on the basis of the $d_{\alpha N}$(77,78) and $d_{\beta N}$(77,78) connectivities identified in Figure 8, are linked by HOHAHA α–β and β–β connectivities, Figure 4.

Assignments of Residues 110–116. Earlier we assigned the K110NH to 7.54 ppm, and connectivities in Figures 6, 7c, and 13 show that the K110α shift is 5.10 ppm. The K110α–V111NH connectivity, Figure 10b, and the Val spin system identifications yield the V111 assignment. the Y113NH assignment and the A112β–Y113NH and A112 N–β connectivities yield the A112NH assignment. The A112 and Y113 α-proton shifts follow from the Ala and Tyr spin system identifications. Similar reasoning leads to the assignments of V114 and Y115 from connectivities observed in Figures 7a, 10b, and 8. The K116NH assignment is based upon the $d_{\alpha N}$(115,116) connectivity identified in Figure 8 and the fact that this NH shift matches an available Lys NH shift observed in the HMQC spectrum of Nase labeled with [^{15}N]Lys, Figure 1Se.

Assignments of Residues 118–121. The assignment of H121NH has been reported (Torchia et al., 1988b) and the H121α is assigned to 5.43 ppm on the basis of H121 N–α connectivities identified in Figures 5 and 8. A Thr carbonyl carbon shows long-range correlations (Bax et al., 1988) to its α-proton, 3.86 ppm, and to another α-proton, 5.43 ppm. This latter correlation must be to H121α because the only other α-proton at 5.43 ppm is that of K24 and this residue is not adjacent to a Thr residue. The assignment of the T120α to 3.86 ppm together with the Thr spin system identifications show that the T120NH is at 10.68 ppm. Residues 118–121 are linked by sequences of $d_{\alpha N}$, $d_{N\alpha}(i,i)$, and d_{NN} connectivities identified in Figures 8 and 12. The N118 and N119 NH–α and ^{15}N–NH correlations are identified in Figures 6 and 1Sa, respectively.

Assignments of Residues 138–141. The W140 protons have been assigned herein, the S141NH has been assigned (Torchia et al., 1988b), and the I139NH is assigned by elimination as all other Ile NH protons are assigned. These assignments are confirmed by the 139–140 and 140–141 d_{NN} connectivities identified in Figure 7a. The I139 N–α connectivity in Figure 6 confirms the identification of I139 N–α connectivity in Figure 7a. The N138α–I139NH connectivity in this figure provides the N138α assignment, and Figure 8 shows intense connectivities between the L137 and N138 α-protons and an NH at 9.04 ppm assigned to N138. The N138 N–α and ^{15}N–NH connectivities are identified in the PS COSY spectrum, Figure 6, and the HMQC spectrum of Nase labeled with [^{15}N]Asx, Figure 1Sa.

Assignments of Residues 6–10. Our above assignment of L25NH also provides the assignment of L7NH, 8.24 ppm, by elimination (Torchia et al., 1988b). The L7NH–K6α cross-peak is identified in Figure 7b; the L7 α-proton assignment is based upon the PS COSY connectivity and the Leu7 ^{15}N–^{1}H connectivity observed in the HMBC spectrum of Nase labeled with [^{15}N]Leu (Bax et al., 1988). The HMQC spectrum of Nase labeled with [1-^{13}C]Leu/[^{15}N]His, Figure 2b, provides the assignment of the H8NH, 8.76 ppm. This result and the PS COSY spectrum show that the only possible H8α assignment is 4.92 ppm. The H8α–K9NH and K9 N–α connectivities are identified in Figure 7c, and the latter assignment is enforced by the K9 N–α connectivity in the PS COSY spectrum. The K9 α-proton has a strong connectivity with an NH at 9.38 ppm, Figure 8, which is assigned to K9α–E10NH because there is an available NH at this position in the [^{15}N]Glx HMQC spectrum. The Glu10 N–α connectivities are identified in Figures 5S, 6, and 8.

Assignments of Residues 50–55. The V51NH is assigned by elimination and the V51 α-proton assignment follows from the Val spin system identifications. The V51NH assignment together with the known Gly α-proton shifts enable us to identify the G50α–V51NH connectivities in Figure 10b, and the G50NH assignment follows from the Gly spin system identifications. The assignment of the E75NH proton implies, by elimination (Torchia et al., 1988b), that the shift of the E52NH is 8.22 ppm. Figures 6 and 7c show that the E52α shift is 4.43 ppm, and $d_{N\alpha}(i,i)$ and $d_{\alpha N}$ connectivities linking E52, K53, and Y54 are identified in Figure 7a,c. By elimination, the NH of G55 is either at 8.91 or at 8.83 ppm and is assigned the latter value because an amide proton at this position has a d_{NN} connectivity with the Y54NH, Figure 12. The G55α assignments follow from the Gly spin system identifications. The Gly55 assignments provide the Gly20 assignments by elimination.

Assignments of Residues 44–46. The H46NH proton is assigned by elimination, as all other His NH protons have been assigned. The weak H46 NH–β connectivity observed in Figure 7b is confirmed by the H46 NH–β connectivities identified in Figure 8. The corresponding H46 α–β connectivities are identified in the HOHAHA spectrum, Figure 4. These H46 assignments are enforced by connectivities observed in the HMBC spectrum of Nase labeled with [^{15}N]His (Bax et al., 1988). The K45α–H46NH and T44[1-^{13}C]/K45α connectivities identified, respectively, in Figure 7c and in the HMBC spectrum of [1-^{13}C]Thr-labeled Nase (Bax et al., 1988), provide the K45α assignment.

Assignments of R81, T82, and D83. By elimination, the unique Thr α-proton at 5.55 ppm must be assigned to T44 or T82. This α-proton has a strong NOESY connectivity with an amide proton at 8.82 ppm. This connectivity is assigned to T82α–D83NH rather than to T44α–K45NH, because there is an unassigned amide NH at 8.82 ppm in the HMQC spectrum of Nase labeled with [^{15}N]Asx but not in the spectrum of Nase labeled with [^{15}N]Lys. The R81 connectivity in Figure 9 is assigned by elimination because all other Arg NH protons have been assigned and the R81 connectivity is not observed in any of the HMQC spectra of Nase labeled with individual types of amino acids. The above assignments are enforced by the d_{NN}(81,82) connectivity identified in Figure 12.

Discussion

The sequential assignments are listed in Table III, and the sequential connectivities upon which the assignments are based are summarized in Figure 14. As has been noted previously, the residues in the three long sequences of d_{NN} connectivities are in good correspondence with the residues in the three α-helical domains identified in the crystal structure of Nase. In addition, we observe many strong $d_{\alpha N}$ connectivities in sequences consisting of residues 7–18, 22–28, 32–41, 71–80, 85–96, and 109–116. These sequences include the β-strands identified in the Nase crystal structure. The sets of long-range NOESY α–α connectivities (9–75, 11–73), (22–35, 24–33), (39–111, 41–109), (72–94, 74–92, 76–90), Figure 15, identify four regions of antiparallel β-structure also present in the crystal structure. In addition many other long-range connectivities [$d_{NN}(i,j)$, $d_{N\alpha}(i,j)$, $d_{Naromatic}(i,j)$] are identified in the NOESY spectra of Nase, Figures 7, 8, and 12. Examination of the X-ray coordinates shows that all these connectivities are between pairs of protons in nonsequential residues i and j having $r(i,j) < 4$ Å, where $r(i,j)$ is the distance between the pair of protons in residues i and j. On the basis of these observations we conclude that conformations of the polypeptide backbone are essentially the same, in the solution and in the crystalline states, throughout most of the protein. However, the backbone conformation of residues 42–49 appears to be flexible in solution. We have observed virtually no d_{NN} and $d_{\alpha N}$ connectivities for these residues, in spite of the fact that many short d_{NN} and $d_{\alpha N}$ distances are found in this region of the sequence in the crystal structure. Because few sequential NOE connectivities are observed for residues 42–49, the only asssigned amide signal in this section of the sequence is that of His46. Therefore, Lys45, -48, and -49 amide signals remain unassigned in spite of the fact that amide HMQC signals of all Lys residues are observed, Figure 1Se. Furthermore, an attempt to assign E43, by labeling Nase with [^{15}N]Z/[1-^{13}C]P, failed. Presumably the E43 amide signal is broad, and the ^{15}N–^{13}C splitting is not seen in the HMQC spectrum, Figure 1Sa. It is noteworthy that the crystallographic b factors are larger than average in this region of the sequence (Professor

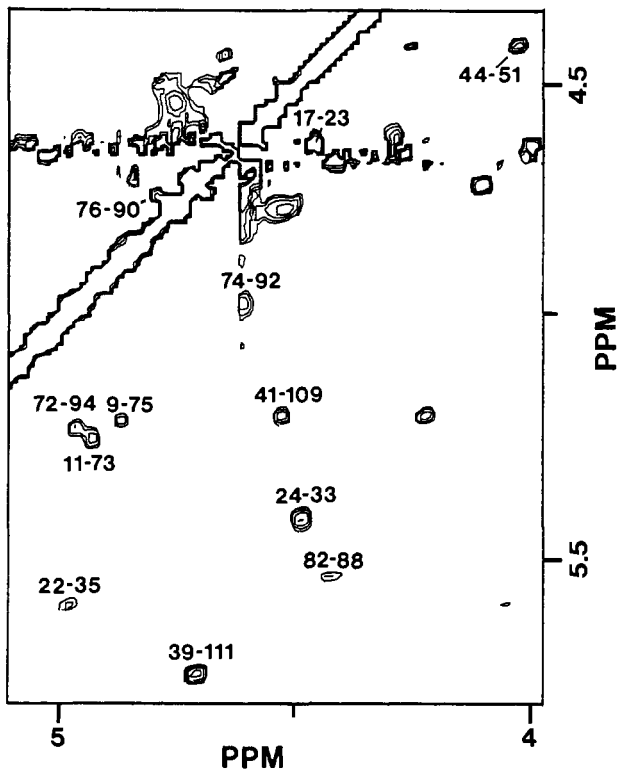

FIGURE 15: 500-MHz NOESY spectrum of deuterium-exchanged Nase: mixing time, 100 ms; pH 7.4. Long-range $d_{\alpha\alpha}$ connectivities, characteristic of antiparallel β-sheet structures, are labeled.

Eaton Lattman and Dr. Philip Loll, Johns Hopkins University, private communication); hence, it is likely that this region of the Nase backbone is flexible in solution. If molecular motions have rates in the 0.1–1-kHz range, NMR signals may be broad. If this is the case, NOESY connectivities will be difficult to detect.

Information about backbone motions on a much slower time scale comes from NH exchange rates that are derived from Figures 9, 13a, and 6S. Comparison of Figures 9 and 13a shows that saturation of the water peak decreases the intensity of relatively few residues (e.g., G20, T33, and M98) in the nonterminal portion of Nase. In contrast, comparison of Figures 13 and 6S, shows that only about 45 amide NH protons remain unexchanged 24 h after Nase is dissolved in ^2H_2O. The first observation shows that nearly all backbone amide protons have exchange rates that are considerably smaller than $1/T_1$ (ca. 1 s^{-1}) at pH 6.5 and 37 °C, whereas only the amide protons of the residues identified in Figure 13a have exchange lifetimes in excess of 8 h. We note that signals from ca. 80% of these amide protons are observed in a spectrum, not shown, recorded after the sample had been stored at 8 °C for 3 months. The protein domains that contain the slowly exchanging protons are depicted in Figure 16. As expected, all of the slowly exchanging amides are hydrogen bonded in the crystal structure. However, it is noteworthy that not all hydrogen-bonded amide protons are slowly exchanging. For instance, Figures 13a and 15 show that only three amide protons in the helix spanning residues 122–134 exchange slowly and only amides in the C-terminal half of α-helix 58–69 exchange slowly. Therefore, although both NMR and X-ray diffraction experiments show that the three helical domains in Nase are well-formed structures, the three helices have significantly different stabilities against hydrogen exchange, with helix 99–109 having the greatest long-term stability.

The slowly exchanging amide protons found outside the α-helices are located in β-strands and antiparallel β-sheets.

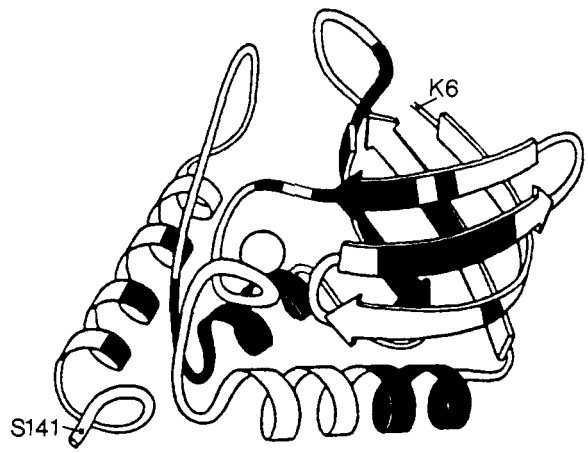

FIGURE 16: Schematic ribbon representation of the Nase backbone (Richardson, 1981) derived from the X-ray structure (Cotton et al., 1979). Shaded regions of the drawing show the locations of the slowly exchanging amide protons.

The β-strand, 87–94, forms part of the pdTp binding pocket and appears to have a particularly stable structure. Not only do all amide protons in this sequence exchange slowly, but the δ-protons of Tyr91 have observably different chemical shifts, Figure 10a, presumably as a consequence of slow Tyr ring flips. No other Tyr or Phe residue in Nase shows evidence of slow flipping. In addition, the OH of Tyr91 exchanges sufficiently slowly in H_2O solution that we can identify NOESY connectivities between this proton and Y91ϵ, T120NH, and H121NH, Figure 12. The Y91OH is the only hydroxyl proton that we have been able to identify.

The assignments presented in Table III provide a starting point for assigning the remaining side-chain protons in Nase by edited NOESY and 3D spectra of ^{15}N-labeled samples together with NOESY and HOHAHA of partially deuteriated samples. The assignments will also permit detailed studies of the effects of ligand binding, site mutations, and other important variables on the structure and dynamics of many specific sites in the protein. It appears that such studies can be also be made on Nase crystals because many chemical shifts in solution and in the crystalline state are observed to be nearly the same (Cole et al., 1988). Finally, the methods used herein should prove useful to other investigators interested in applying NMR approaches to study the structure and dynamics of proteins having M_r greater than 10K.

ACKNOWLEDGMENTS

We thank Professor John Gerlt for the transformed *E. coli*, Professor Paul Young for the labeled leucine and threonine amino acids, and Rolf Tschudin for expert technical support. We are grateful to Professor Eaton Lattman and Dr. Philip Loll for providing us with the X-ray coordinates of the Nase/pdTp/Ca^{2+} complex prior to publication and to Dr. Bernard Brooks of the National Institutes of Health for converting the coordinates into internuclear distances.

SUPPLEMENTARY MATERIAL AVAILABLE

Tables IS and IIS listing assignments of Nase residues in flexible terminal domains; Figure 1S showing ^1H–^{15}N HMQC spectra of Nase labeled with (a) [1-^{13}C]P/[^{15}N]Z, (b) [1-^{13}C]K/[^{15}N]G, -I, -S, and -Y, (c) [1-^{13}C]M/[^{15}N]T and -Y, (d) [1-^{13}C]I/[^{15}N]Y, and (e) [1-^{13}C]A/[^{15}N]K and -Y; Figure 2S showing ^1H–^{13}C HMQC spectra of Nase labeled with (a) [2-^{13}C]G and -S, (b and c) [3,4-$^{13}C_2$]T, and (d) [2-^{13}C]P; Figure 3S showing NOESY spectrum depicting W140 connectivities in the amide–aromatic region of the spectrum;

Figure 4S showing NOESY spectrum of deuteriated Nase showing B, Z, and W connectivities in the amide–aliphatic region of the spectrum; Figure 5S showing ^{15}N-edited NOESY spectra of Nase labeled with (a) [^{15}N]F, (b) [^{15}N]M, and (c) [^{15}N]T and -Y; and Figure 6S showing ^{1}H–^{15}N HMQC spectrum of ^{15}N-labeled Nase, recorded with water presaturation (14 pages). Ordering information is given on any current masthead page.

References

Alexandrescu, A. T., Mills, D. A., Ulrich, E. L., Chinami, M., & Markley, J. L. (1988) *Biochemistry 27*, 2158–2165.

Bax, A., & Lerner, L. (1986) *Science 232*, 960–967.

Bax, A., Griffey, R. H., & Hawkins, B. L. (1983) *J. Magn. Reson. 55*, 301–315.

Bax, A., Sparks, S. W., & Torchia, D. A. (1988) *J. Am. Chem. Soc. 110*, 7926–7929.

Bax, A., Kay, L. E., Sparks, S. W., & Torchia, D. A. (1989) *J. Am. Chem. Soc. 111*, 408–409.

Bendall, M. R., Pegg, D. T., & Doddrell, D. M. (1983) *J. Magn. Reson. 52*, 81–117.

Calderon, R. O., Stolowich, N. J., Gerlt, J. A., & Sturtevant, J. M. (1985) *Biochemistry 24*, 6044–6049.

Cole, H. B. R., Sparks, S. W., & Torchia, D. A. (1988) *Proc. Natl. Acad. Sci. U.S.A. 85*, 6362–6365.

Cotton, F. A., Hazen, Jr., E. E., & Legg, M. J. (1979) *Proc. Natl. Acad. Sci. U.S.A. 76*, 2552–2555.

Cross, T. A., & Opella, S. J. (1985) *J. Mol. Biol. 182*, 367–381.

Ernst, R. R., Bodenhausen, G., & Wokaun, A. (1987) *Principles of Nuclear Magnetic Resonance in One and Two Dimensions*, Clarendon Press, Oxford.

Evans, P. A., Dobson, C. M., Kautz, R. A., Hatfull, G., & Fox, R. O. (1987) *Nature 329*, 266–270.

Fesik, S. W., Luly, J. R., Erickson, J. W., & Abad-Zapatero, C. (1988) *Biochemistry 27*, 8297–8301.

Fox, R. O., Evans, P. A., & Dobson, C. M. (1986) *Nature 320*, 192–194.

Griffey, R. H., & Redfield, A. G. (1987) *Q. Rev. Biophys. 19*, 51–82.

Griffey, R. H., Redfield, A. G., Loomis, R. E., & Dahlquist, F. W. (1985) *Biochemistry 24*, 817–822.

Griffey, R. H., Redfield, A. G., McIntosh, L. P., Oas, T. G., & Dahlquist, F. W. (1986) *J. Am. Chem. Soc. 108*, 6816–6817.

Gronenborn, A. M., Bax, A., Wingfield, P., Clore, G. M. (1988) *FEBS Lett. 243*, 93–98.

Hibler, D. W., Stolowich, N. J., Reynolds, M. A., Gerlt, J. A., Wilde, J. A., & Bolton, P. H. (1987) *Biochemistry 26*, 6278–6286.

Howarth, O. W., & Lilley, D. M. J. (1978) *Prog. Nucl. Magn. Reson. Spectrosc. 12*, 1–40.

Kainosho, M., & Tsuji, T. (1982) *Biochemistry 21*, 6273–6279.

Leighton, P., & Lu, P. (1987) *Biochemistry 26*, 7262–7271.

LeMaster, D. M., & Richards, F. M. (1988) *Biochemistry 27*, 142–150.

Lerner, L., & Bax, A. (1986) *J. Magn. Reson. 69*, 375–380.

Marion, D., & Wuethrich, K. (1983) *Biochem. Biophys. Res. Commun. 113*, 6394–6396.

McIntosh, L. P., Griffey, R. H., Muchmore, D. C., Nielson, C. P., Redfield, A. G., & Dahlquist, F. W. (1987) *Proc. Natl. Acad. Sci. U.S.A. 84*, 1244–1248.

McIntosh, L. P., Dahlquist, F. W., & Redfield, A. G. (1988) *J. Biomol. Struct. Dyn. 5*, 21–34.

Muchmore, D. C., McIntosh, L. P., Russell, C. B., Anderson, D. E., & Dahlquist, F. W. (1989) *Methods Enzymol.* (in press).

Mueller, L. (1979) *J. Am. Chem. Soc. 101*, 4481–4484.

Oh, B. H., Westler, W. M., Darba, P., & Markley, J. L. (1988) *Science 240*, 908–911.

Redfield, C., & Dobson, C. M. (1988) *Biochemistry 27*, 122–136.

Richardson, J. S. (1981) *Adv. Protein Chem. 34*, 167–339.

Roy, S., Redfield, A. G., Papastavros, M. Z., & Senchex, V. (1984) *Biochemistry 23*, 4395–4400.

Senn, H., Otting, G., & Wuethrich, K. (1987) *J. Am. Chem. Soc. 109*, 1090–1092.

Serpersu, E. H., Shortle, D., & Mildvan, A. S. (1987) *Biochemistry 26*, 1289–1300.

Shortle, D. (1983) *Gene 22*, 181–189.

Shortle, D., & Lin, B. (1985) *Genetics 111*, 539–555.

Sklenar V., & Bax, A. (1987) *J. Magn. Reson. 74*, 469–479.

Smith, S. O., & Griffin, R. G. (1988) *Annu. Rev. Phys. Chem. 34*, 511–535.

States, D. J., Haberkorn, R. A., & Ruben, D. J. (1982) *J. Magn. Reson. 48*, 286–292.

Torchia, D. A., Sparks, S. W., & Bax, A. (1988a) *J. Am. Chem. Soc. 110*, 2320–2321.

Torchia, D. A., Sparks, S. W., & Bax, A. (1988b) *Biochemistry 27*, 5135–5141.

Tucker, P. W., Hazen, E. E., & Cotton, F. A. (1978) *Mol. Cell. Biol. 22*, 67–77.

Tucker, P. W., Hazen, E. E., & Cotton, F. A. (1979a) *Mol. Cell. Biol. 23*, 3–16.

Tucker, P. W., Hazen, E. E., & Cotton, F. A. (1979b) *Mol. Cell. Biol. 23*, 67–86.

Tucker, P. W., Hazen, E. E., & Cotton, F. A. (1979c) *Mol. Cell. Biol. 23*, 131–141.

Westler, W. M., Kainosho, M., Nagao, H., Tomonaga, N., & Markley, J. L. (1988) *J. Am. Chem. Soc. 110*, 4093–4095.

Wuethrich, K. (1986) *NMR of Proteins and Nucleic Acids*, Wiley, New York.